Extreme Responses and Associated Uncertainties for a Long End-Anchored Floating Bridge

Zhengshun Cheng[a,b,*], Zhen Gao[c], Torgeir Moan[c]

[a] *State Key Laboratory of Ocean Engineering, Shanghai Jiao Tong University, Shanghai 200240, China*
[b] *SJTU Yazhou Bay Institute of Deepsea Science and Technology, Sanya 572024, China*
[c] *Department of Marine Technology and Centre for Autonomous Marine Operations and Systems (AMOS), Norwegian University of Science and Technology (NTNU), Trondheim, 7491, Norway*

Abstract

Very-long floating bridges represent an innovative marine structure for crossing wide and deep fjords. During the design of a floating bridge, extreme structural responses at a specified probability of exceedance are required to be properly evaluated for ultimate limit state (ULS) design check. This study addresses the estimation of extreme structural responses due to wind and wave loads and associated uncertainties. An end-anchored floating bridge, about 4600 m, is considered in a case study. The long-term extreme responses are estimated by using a simplified engineering approach, in which the long-term extreme response is approximated by the one-hour short-term extreme responses at a high fractile (90% in this study) for selected short-term sea states. The extreme responses are expressed as $\mu + \kappa \cdot \sigma$, where μ and σ are the ensemble mean and standard deviation, and κ is a multiplying factor. Statistical analyses indicate that the structural responses, including axial force , strong and weak axis bending moment of the bridge girder, are close to follow a Gaussian distribution. A simplified analytical method, the Gumbel method and the mean upcrossing rate (MUR) method are employed to estimate the multiplying factor κ and extremes. The κ estimated by these three methods are generally close, varying in the vicinity of 4. The κ and extremes estimated by the simplified method have a much smaller variation than the Gumbel and MUR methods. Statistical uncertainties and model uncertainties in the extreme value prediction are also addressed. Based on the results of 10 sets of 10 1-h ensembles, the mean and coefficient of variation (CoV) of μ, κ, σ and extremes of structural responses of 10 1-h simulations under two selected sea states are evaluated. The CoV of σ is less than 0.045, but the CoV of κ is relatively large, mainly between 3.5×10^{-2} and 6.5×10^{-2}. The CoV of extremes estimated by the simplified analytical method is fairly small, less than 0.035. While the CoV of extremes estimated by the Gumbel and MUR methods are much larger and can reach 0.137 and 0.158, respectively. In practical design of floating bridge, only a limited number of simulations (e.g. 10 1-h) are conducted to predict the extreme structural responses. This will introduce statistical uncertainties and should be corrected by a factor for a conservative estimate. A simplified procedure to derive the correction

factor is presented in this study. For the floating bridge considered with 10 1-h simulations, the correction factor is recommended to be 1.1 when the absolute value of mean μ is smaller than σ, and be 1.2 when the absolute value of mean μ is larger than σ, in order to achieve a 90% conservative estimation of extreme.
Keywords: floating bridges, extreme responses, uncertainties, environmental contour method, correction factor

1. Introduction

Upgrading of the Coastal-Highway Route E39 project is presently being planned by the Norwegian Public Roads Administration (NPRA). This includes replacement of ferry transport across 8 fjords by bridges or tunnels. The width of the fjord crossings is up to 6 kilometers and the water depth is up to 1300 m. Due to the large width, traditional free span for bridges with towers on land will have excessive and very expensive spans. Moreover, because of the large water depth, bridges with bottom-fixed foundations in the fjords are not economical. Therefore a promising alternative is to employ floating bridges. Currently several floating bridge concepts have been proposed for crossing deep and wide fjords, including an end-anchored curved floating bridge, an side-anchored straight floating bridge, etc. [1]

Compared to floating offshore structures, floating bridges are relatively flexible with a large number of eigen-modes. These eigen-modes may be excited by environmental loads, which can cause large structural responses. Characteristics of dynamic behavior of extra-long floating bridges have been studied under homogeneous [2, 3, 4] and inhomogeneous [5] environmental conditions.

During the design of offshore structures, characteristic values of long-term extreme load effects are required to carry out ultimate limit state (ULS) design checks [6]. To predict the long-term extreme load effects due to environmental loads, a full long-term approach should in principle be used to account for the variation of environmental conditions. The long-term variation in wind and wave conditions is usually considered by assuming sequential stationary short-term conditions. Since wind in 10 minutes and waves in 3 hours are normally considered as stationary, a duration of one hour is commonly employed as a alternative for short-term wind and wave conditions. The full long-term approach should account for all possible combination of short-term environmental conditions and their probability of occurrence. This implies that a very large number of short-term simulations have to be carried out. For complex structures like extra-long floating bridges, each

*Corresponding author.
Email address: zhengshun.cheng@sjtu.edu.cn; zhengshun.cheng@gmail.com

short-term simulation is commonly very time consuming. The full long-term approach is often considered infeasible in engineering design.

Approximate methods are thus proposed for predicting the long-term extreme load effects. A commonly used approach is the environmental contour method [7, 8], in which the long-term extreme response for a return period of N-year is approximated by the extreme from few short-term analyses. In this approach, the N-year contour surface (or contour line when two environmental variables are considered) should be first constructed based on the long-term joint distribution of environmental parameters, such as mean wind speed, significant wave height and peak period. The most severe sea state that cause the largest short-term extreme responses is then identified from the N-year contour surface. Compared to a full long-term approach, the environmental contour method requires only a few short-term simulations, making it very efficient and suitable for use in the practical design of offshore structures. However, the variability of short-term extremes should be taken into account when using the environmental contour method. This is usually achieved by multiplying a correction factor (1.1-1.3) [9] or by determining the short-term extreme responses at a higher quantile (75-90%) [10, 11]. The exact value of the correction factor or the quantile is required to be calibrated by a full long-term analysis.

Many studies have been conducted to estimate extreme responses of floating platforms [12, 13], bottom-fixed offshore wind turbines [14] and floating wind turbines [15]. However, to date, there are few studies on the estimation of extreme responses for floating bridges. Øiseth et al. [16] estimated the extreme response of a floating bridge by using Monte Carlo simulations. The extreme value was extrapolated by using the average conditional exceedance rate method, in which a high quantile of 85% was assumed and used. Giske et al. [17] demonstrated a framework for full long-term extreme response analysis for a long-span pontoon bridge subjected to wave loads, by using inverse first- and second-order reliability methods (IFORM and ISORM). Xu et al. [18] introduced a computationally efficient approach utilizing the environmental contour method and the IFORM to determine the long-term extreme responses of a cable-supported bridges with floating pylons due to wind and wave actions. The quantile used in the environmental contour method was calibrated to be 90%. However, the long-term environmental conditions used by Xu et al. [18] were originally developed for open sea, not for a fjord.

In addition, uncertainties exist in the prediction of extreme responses. These uncertainties need to be considered when assessing the safety of a structure. Moan et al. [19] investigated the statistical uncertainties in the predicted extreme responses of an FPSO and a semi-submersible due to long-term variation of wave conditions in consecutive 1, 2 and 4-year periods. Saha et al. [14] evaluated the statistical uncertainties in the predicted 3-hour extreme responses of a jacket-type offshore wind turbine due to ensemble size, by using different extrapolation methods, including the Gumbel method, the mean upcrossing rate method and the Weibull tail method.

The aim of this paper is to evaluate the extreme structural responses and associated uncertainties of an end-anchored curved floating bridge. The long-term extreme response is estimated by using a simplified environmental contour method, in which the long-term extreme value is approximated by the short-term extreme value at a high quantile. The short term response is obtained by time domain simulations and the extreme values are estimated by an approximate analytical approach and two methods based on response fitting and extrapolation techniques. The uncertainty in the predicted extreme responses is also addressed comprehensively.

2. Floating bridge model

An end-anchored floating bridge is considered in this study. It was an early concept for crossing the Bjørnafjord. An over view of the floating bridge is shown in Fig. 1. The floating bridge, about 4600m long, is curved in the horizontal plane with a radius of approximately 5000m. It composes of a cable-stayed high bridge part and a pontoon-supported low bridge part. The high bridge part is designed for ship navigation and consists of a main span of 490m and a back span of 370m. The bridge girder is carried by 80 cables in the high bridge part, while in the low bridge part, the bridge girder is supported by 19 pontoons with a span of about 197m through columns.

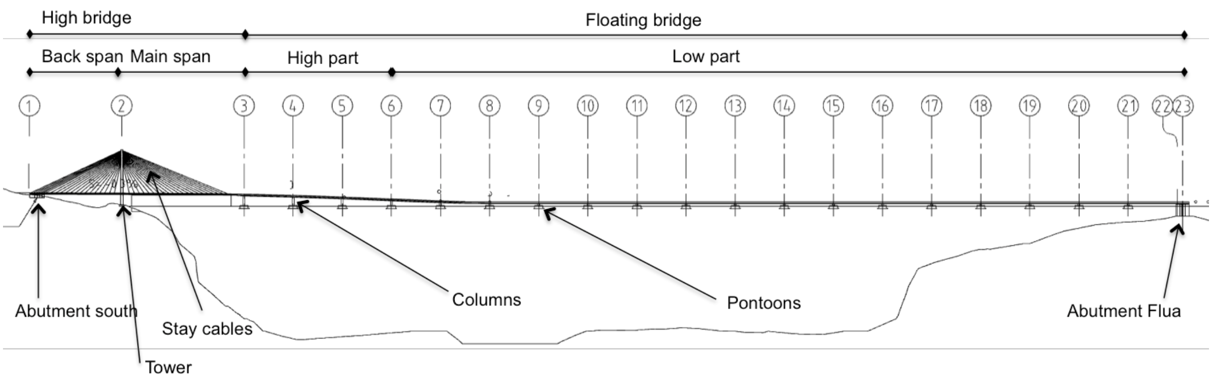

Figure 1: Overview of the end anchored curved floating bridge concept [20].

A numerical model of the floating bridge, as demonstrated in Fig. 2, was established by using the codes SIMO/RIFLEX developed by SINTEF OCEAN (formerly MARINTEK). The SIMO/RIFLEX has been widely used in the offshore oil & gas and wind industries. The structural modeling of the floating bridge is briefly introduced here, while the external load models are discussed in the next section. In this study, the girder, tower, and columns were modeled as nonlinear beam elements. The cables were represented as nonlinear bar elements, while the pontoons were modeled as floating rigid bodies with 6 degree of freedom (DOF) each. For the mesh size, the element length varies from 10 m to 15 m for the girder, from 5 m to 8 m for the columns, and from

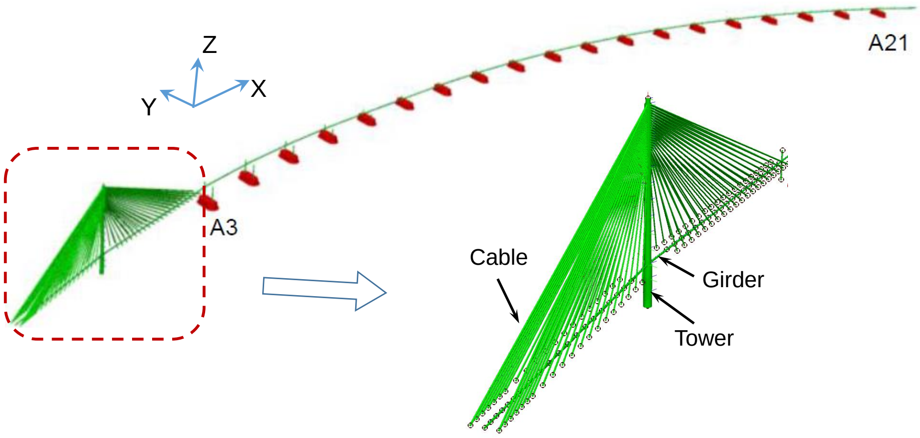

Figure 2: The end anchored curved floating bridge model including a cable stayed high bridge and a pontoon supported low bridge [2].

30 m to 40 m for the cables, depending on the locations. The dynamic equilibrium equations are solved in the time domain using the Newmark-β numerical integration, in which the required accuracy measured by energy norm is 10^{-6}. The structural properties of typical sections of the bridge girder are given in Table 2, in which the location of typical sections are indicated in Table 1. Here the detailed properties of the columns, cables and tower are not presented, but they are described in the report [20], which is publicly available online.

Table 1: Location of different cross-sectional properties for the bridge girder [20]. Here H1, H2, H3, S1 and F1 represent different cross sections, and the corresponding properties are given in Table 2.

Cross-section	Roadline
Stiff bridge (abutment)	S=0m to S=60m
H1	S=60m to S=220m
H2	S=220m to S=345m
H3	S=345m to S=395m
H2	S=395m to S=520m
H1	S=520m to S=850m
S1	S=850m to S=860m
S1(24.62m) - F1(147.74m) - S1(24.62m)	S=860m to S=4602.74m

In the numerical model, the tower bottom and two ends of the bridge are fixed. The bridge girder and the tower are connected by a point with fixed degree of freedom in transverse direction (i.e. Y direction as shown in Fig. 4). Master-slave rigid connection is applied between pontoons and columns, between girder and cable lower ends, and between girder and columns. Moreover, the pretension in each cable is accounted for in the numerical model. It should be noted that in the numerical model, the bridge girder that is composed of two parallel steel boxes connected by

Table 2: Structural properties of the bridge girder [20]

		High bridge			Floating bridge	
		H1	H2	H3	S1	F1
Mass	$[ton/m]$	23.96	29.05	33.13	31.8	26.71
EA	$[kN]$	3.07E+08	4.41E+08	5.52E+08	5.25E+08	3.89E+08
EI_z	$[kNm^2]$	1.16E+11	1.70E+11	2.12E+11	2.18E+11	1.55E+11
EI_y	$[kNm^2]$	1.28E+09	1.97E+09	2.46E+09	3.85E+09	2.76E+09
GI_x	$[kNm^2]$	1.42E+09	1.98E+09	2.48E+09	3.70E+09	2.90E+09

Note that I_y and I_z represent the second area moment about the strong axis and weak axis of the girder, respectively. I_x denotes the torsion constant.

crossbeams in the original design is simplified as an equivalent beam.

The floating bridge is relatively flexible, with a large number of eigen-modes. The eigen-periods and eigen-modes of the floating bridge was studied by Cheng et al. [2], as demonstrated in Fig. 3. The first four eigen-periods are given in Table 3. The global coordinate system is defined in Fig. 4. X is positive in the north direction, and Y is positive in the west direction. and Z is positive upward. The origin is located at the water plane and is 2250m North of the south end. The incoming directions of wind, wave and current are also marked in Fig. 4.

Table 3: The first four eigen periods of the floating bridge model.

Mode	Period [20] [s]	Frequency [20] [rad/s]	Dominant motion	Period [2] [s]	Error [%]
1	56.72	0.111	H	55.52	2.12
2	31.69	0.199	H	31.81	-0.38
3	22.68	0.277	H	23.07	-1.72
4	18.62	0.337	H	19.04	-2.26

3. Methodology

3.1. Fully coupled analysis method

Fully coupled aero-hydro-elastic time-domain simulations are conducted to investigate the dynamic behavior of the floating bridge in this study. The hydrodynamic loads on the pontoons and the aerodynamic loads on the structures as well as the structural dynamics are accounted for.

The structural dynamics are modeled in RIFLEX [21]. RIFLEX is a nonlinear finite element solver. It represents the cables by nonlinear bar elements, models the bridge girder, tower and columns by nonlinear beam element, and represents the pontoons as floating rigid bodies.

The aerodynamic loads acting on structures, including the bridge girder, columns, tower and cables, are also modeled in RIFLEX. The aerodynamic loads are estimated based on the relative velocity between wind and structures. The aerodynamic loads on columns, tower, and cables are mainly viscous drag forces. However, the aerodynamic loads on the bridge girder consist of

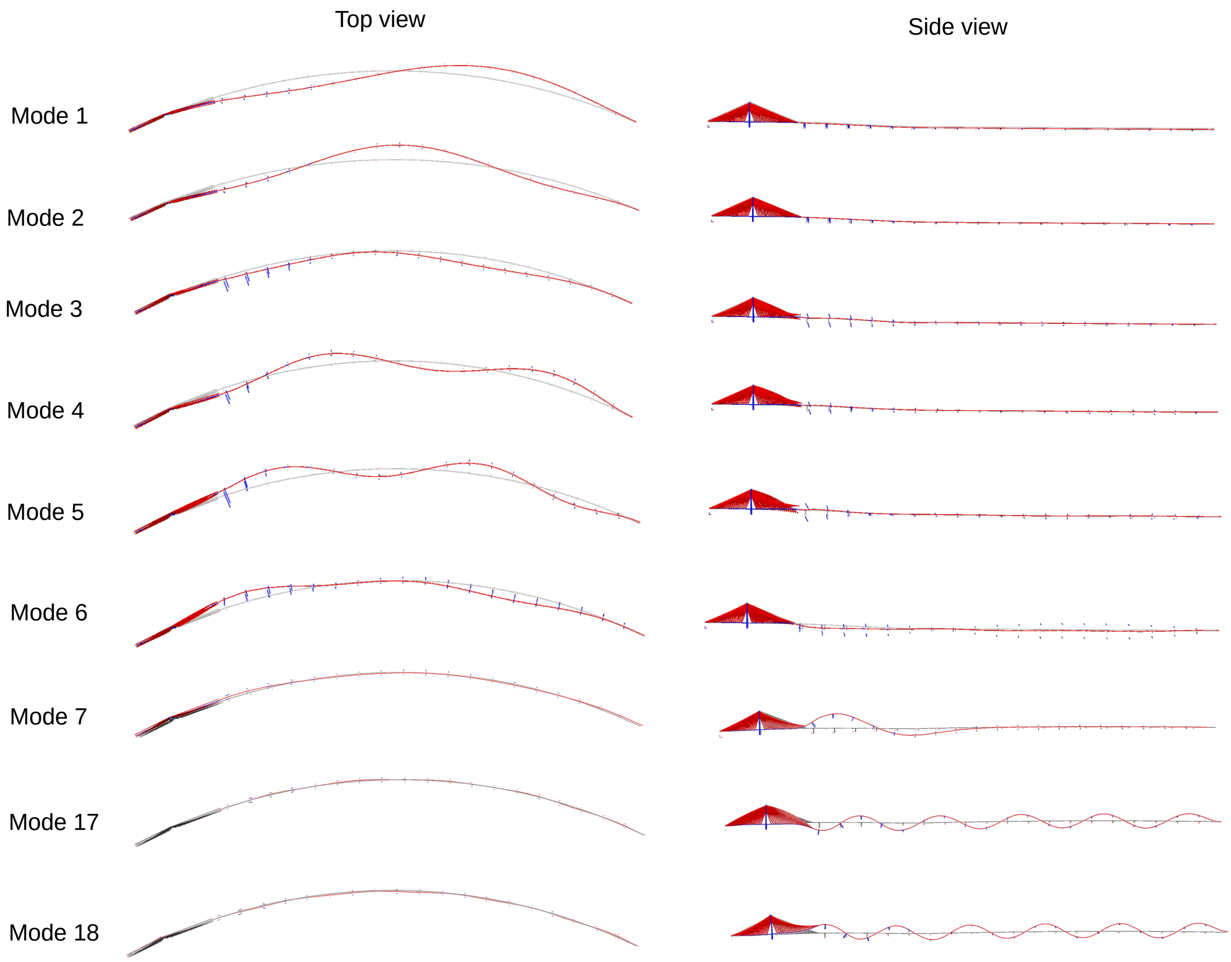

Figure 3: Selected eigen-modes of the floating bridge model [2].

three parts: the mean force due to mean wind velocity, the buffeting force due to fluctuating wind velocity, and the frequency-dependent force induced by girder motion [22]. In the present study, the aerodynamic loads on the bridge girder are estimated by employing the nonlinear quasi-static airfoil theory. This theory considers both aerodynamic lift and drag forces and moment; however, the frequency-dependent forces induced by structure motions are neglected. This nonlinear quasi-static airfoil theory has been used, e.g. by Cheng et al. [3], in analyses of floating bridge design for the Bjørnafjord crossing.

Regarding the hydrodynamic loads on the pontoons, they are considered in SIMO [23] based on a combination of potential flow theory and Morison's equation. Since pontoons are large volume structures, the potential flow theory is thus employed to calculate the frequency-domain hydrodynamic coefficients, such as added masses, radiation dampings, and transfer functions of wave

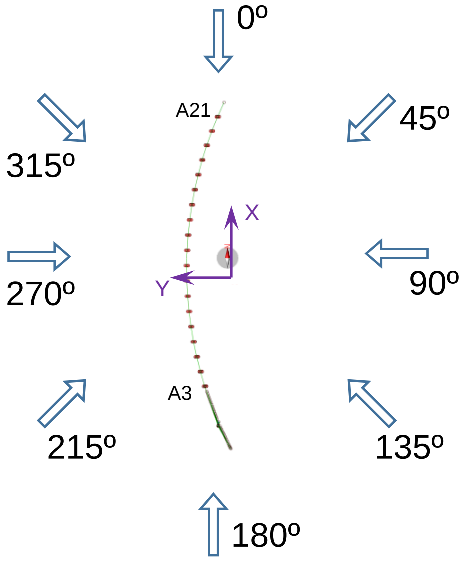

Figure 4: Definition of the global coordinate system and incoming directions of wind, wave and current. Note that the fjord boundary condition is not plotted here.

excitation forces, etc. These hydrodynamic coefficients are then transfered into time domain by using the convolution technique [24]. In the present study, not only first-order wave loads but also second-order wave loads are incorporated. The second-order wave loads are considered by using Newman's approximation. Because of large spacing between adjacent pontoons, the hydrodynamic interactions between adjacent pontoons are not taken into account yet. In addition, viscous drag forces on the pontoons are also accounted for through Morison's equation by including only the quadratic viscous drag term.

3.2. Extreme value estimation

In this study, the long-term extreme response is estimated by the environmental contour method, in which the extreme response is approximated by the short-term extreme responses at a high fractile value. In this approach, the short-term condition considered should be especially selected to be the one that causes the largest short-term extreme responses. The fractile is used to determine the extrapolated extreme responses and is usually determined by comparison with full long-term results. For simplicity in this study, the long-term extreme value of response $X(t)$ is assumed to be expressed as

$$X_{max} = \mu + \kappa \cdot \sigma \tag{1}$$

where μ and σ are the ensemble mean and standard deviation of the time series of short-term responses considered, and κ is a multiplying factor and depends on the selection of the fractile.

The extreme value is the maximum in a set of a finite number of independent and identically distributed random variables. Considering a stochastic process $X(t)$ over a duration $[0, T]$, the extreme value of the stochastic process is defined as $M(T) = \max\{X(t); 0 \leq t \leq T\}$ and the extreme value distribution for large values of y is expressed as

$$F(y) = \mathrm{Prob}\,(M(T) \leq y) \tag{2}$$

Extreme values are commonly evaluated by using extrapolation methods. Besides, if $X(t)$ is a stationary Gaussian process, the extreme value can be approximated by a simplified analytical method. In this section, a simplified analytical method and two extrapolation methods including the Gumbel method and the mean upcrossing rate (MUR) method are briefly described.

3.2.1. Gumbel method

In this method, the cumulative distribution is estimated based on the simulated maxima data. The type I asymptotic extreme value distribution, i.e., the Gumbel distribution, is applied to estimate the extreme value by fitting the simulated cumulative distribution. The extreme value distribution is expressed by

$$F(y) = G_X(y) \tag{3}$$

where $G_X(x)$ is the Gumbel distribution given by:

$$G_X(x) = \exp\left\{-\exp\left[-\left(\frac{x-\beta}{\alpha}\right)\right]\right\} \tag{4}$$

where α and β are scale and location parameters. These two parameters can be estimated by, e.g., least square fitting of the empirical cumulative distribution in a probability paper.

3.2.2. Mean upcrossing rate method

The mean upcrossing rate is a key parameter for extreme response statistics [6]. The upcrossing rate of a process at a defined level is the average frequency of the positive slope crossings of that level. At high response levels, with the assumption of statistically independent upcrossing, it is reasonable to assume that the random number of upcrossing in an arbitrary time interval of length T is approximately Poisson distributed. If the response process is not too narrow banded, this is a reasonable assumption. Then the extreme value distribution is given by

$$F\,(y) = \exp\left(-\int_0^T \nu^+(y;t)dt\right) = \exp\left(-\bar{\nu}^+(y)T\right) \tag{5}$$

where $\nu^+(y;t)$ is the upcrossing rate of the level y. $\bar{\nu}^+(y) = \frac{1}{T}\int_0^T \nu^+(y;t)dt$ is the mean upcrossing rate and can be directly estimated from simulated time series.

For high response levels, the up-crossing rate is low and extrapolation of $\nu^+(y)$ is usually required. In this study, the extrapolation strategy proposed by Naess [12] is employed. The mean up-crossing is extrapolated based on a set of stochastic realizations and is assumed to be in the form of

$$\bar{\nu}^+(y) = q(y)\exp\{-a\,(y-b)^c\}\,, y \geq y_0 \tag{6}$$

in which a, b, c are parameters. For a wide range of dynamic systems, the function $q(y)$ varies slowly compared to the exponential function $\exp\{-a\,(y-b)^c\}$ for tail values of y, it is thus usually replaced by a constant. The optimal values for a, b, c and q are determined by applying the Levenberg-Marquardt least squares optimization method, which is described in detail by Naess [12, 13].

3.2.3. Simplified analytical method

For a stationary Gaussian process $X(t)$ over a duration of T with zero mean, the cumulative distribution of the extreme value is given by Eq. 5, in which the mean up-crossing rate of level y can be approximated by [6]

$$\bar{\nu}^+(y) = \bar{\nu}^+(0)\exp\left(-\frac{y^2}{2\sigma^2}\right) \tag{7}$$

where $\bar{\nu}^+(0)$ is the mean zero up-crossing rate given by

$$\bar{\nu}^+(0) = \frac{1}{2\pi}\sqrt{\frac{m_2}{m_0}} \tag{8}$$

and m_i $(i = 0, 1, 2)$ is the m^{th} moment of the spectral density function of the Gaussian process. $\sigma = \sqrt{m_0}$ is the standard deviation of the Gaussian process. Assuming that a fractile of the extreme value distribution is denoted by ξ, the corresponding level is given by

$$y_\xi\,(T) = \sigma\sqrt{2\ln\left(\frac{\bar{\nu}^+(0)T}{\ln(1/\xi)}\right)} \tag{9}$$

The derived approximation is a Poisson model that is asymptotically exact for large duration T. However, convergence to the Poisson model becomes slow for too narrow-banded processes. To account for the effect of bandwidth, Vanmarcke [25] developed a more accurate model, in which the up-crossing rate of level y is approximated by multiplying a correction factor [26]

$$p(y) = \left(1 - \exp\left[-\left(1 - \alpha_b^2\right)^{0.6} \sqrt{2\pi}\frac{y}{\sigma}\right]\right)\left(1 - \exp\left(-\frac{y^2}{2\sigma^2}\right)\right)^{-1} \tag{10}$$

where $\alpha_b = m_1/\sqrt{m_0 m_2}$ is the bandwidth parameter which tends to one for a narrow-band process. In this case, the extreme value distribution is written as

$$F(y) = \exp\left(-\bar{\nu}^+(0)\exp\left(-\frac{y^2}{2\sigma^2}\right)\cdot p(y)\cdot T\right) \tag{11}$$

In Eq. 11, the level corresponding to a fractile of ξ and a duration T, i.e., y_ξ, cannot be solved directly, an iterative procedure is required. Fig. 5 presents the κ, which is defined as $\kappa = y_\xi/\sigma$, at a fractile of 90% and for a duration of 1 hour. It is a function of bandwidth parameter α_b and zero up-crossing period ($T_z = 1/\bar{\nu}^+(0)$). It can be found that the correction factor $p(y)$ mainly adjust the value of κ when the bandwidth parameter is close to one, in particular $\alpha_b > 0.9$. When α_b is smaller than 0.9, the correction factor has a negligible effect.

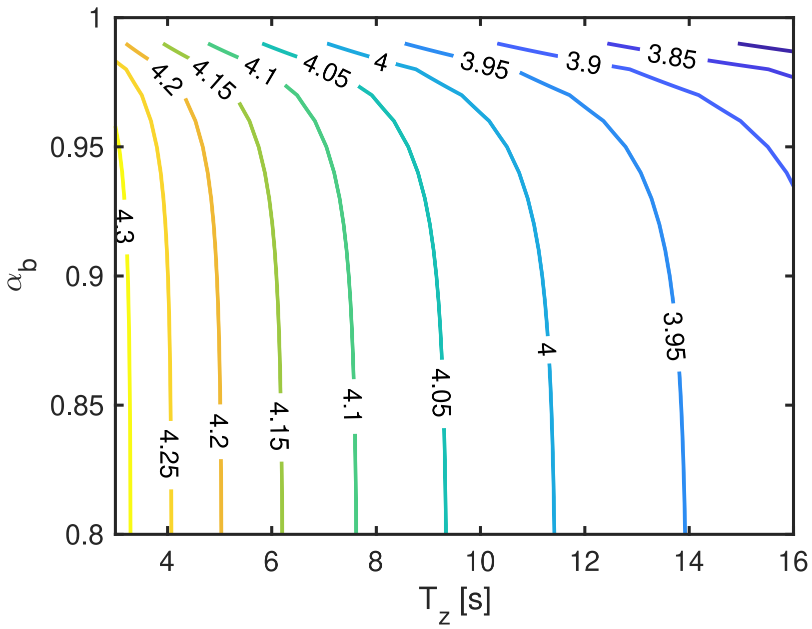

Figure 5: κ as a function of bandwidth parameter α_b and zero crossing period T_z for a fractile of 90% and a duration of 1 hour for the extreme value distribution.

4. Environmental conditions

The short-term environmental conditions should be specially chosen to be the one that leads to the largest extreme responses, i.e., according to the environmental contour method. In this study, these short-term environmental conditions are determined according to an early draft of the metocean design basis for the Bjørnafjord [27], in which wind and wave conditions with a return period of 100 years were defined. The environmental conditions (ECs) as given in Table 4 are considered. EC2 with a combination of 100-year wind and 100-year wave condition is likely to be the worst combined wind and wave condition and is thus selected as the short-term condition for evaluation of long-term extremes. Cheng et al. [28] studied the long-term joint distribution of environmental conditions in the Bjørnafjord and found that the worst condition on the 100-year contour surface of significant wave height H_s, peak period T_p and mean wind speed U_w is fairly close to the 100-year wind condition and the 100-year wave condition. Besides, EC1 with 100-year wave condition is the worst wave only condition. It is also studied to investigate the effect of wave on long-term extremes.

Table 4: Environmental conditions (ECs) for numerical simulations

	Dir. [°]	Wave			Wind	
		H_s [m]	T_p [s]	Spreading (n)	U_w [m/s]	T_I
EC1	270	2.4	5.9	4	0	0
EC2	270	2.4	5.9	4	29.5	0.14

The wind and waves are assumed to be directionally aligned, and only one direction (270°) is considered to demonstrate the methodology. The waves are short-crested and are described by the directional wave spectrum, which is given by

$$S_{\zeta}(\omega, \theta) = S(\omega)D(\theta) \tag{12}$$

where the wave spectrum $S(\omega)$ is modeled by the JONSWAP spectrum and the directional distribution $D(\theta)$ takes the cos-n distribution as follows:

$$D(\theta) = \frac{\Gamma(1 + n/2)}{\sqrt{\pi}\Gamma(1/2 + n/2)} \cos^n \left(\theta - \theta_p\right) \tag{13}$$

where n is the spreading exponent, and is set to be 4 for short-crested waves [27] in this study. θ_p is the principal wave direction and $\left|\theta - \theta_p\right| \leq \pi/2$.

The wind field consists of wind shear and turbulence. The power law formulation of wind shear is applied to describe the vertical distribution of mean wind speed. For wind coming from west (270°), the power law exponent is approximately 0.12. The turbulence intensity for wind coming from west (270°) is about 0.14. In the numerical simulation, the 3D turbulent wind field is generated by the TurbSim [29] based on the N400 Kaimal spectral model [30].

5. Evaluation of extreme responses

In the ULS design check of marine structures, the characteristic long-term extreme response can be approximated as a given fractile of a representative short-term extreme value, based on the environmental contour method. This fractile is used to determine the extrapolated extreme responses and is usually determined by comparison with full long-term results. In this study, a 90% fractile is used, as recommended by the NPRA [27].

The Monte Carlo simulation method is used to generate a set of responses for prediction of extreme responses. A total of 100 1-hour simulations were made for each EC. To investigate the accuracy of a limited ensemble number on the extrapolated extreme responses, the total ensemble is grouped into 2 sets with 50 ensembles, 5 sets with 20 ensembles and 10 sets with 10 ensembles, respectively. For each set, the mean values and standard deviations of structural responses are calculated and the extreme responses are extrapolated by using Gumbel method and mean upcrossing rate (MUR) method, respectively.

Before presenting the results on extreme structural responses, dynamic behavior of the structural responses and their statistics are first addressed.

5.1. Characteristics of structural dynamic responses

The structural dynamic responses of the floating bridge subjected to environmental loads have been extensively studied by Cheng et al. [2, 3]. The main characteristics of structural responses along the bridge girder are briefly summarized here. In general, the structural dynamic responses are mainly dominated by wave- or wind-induced resonant responses as well as wave frequency responses.

To elaborate on this, the dynamic responses of the bridge girder at A6 under EC1 with wave only and EC2 with combined wind and waves are further analyzed here. Fig. 6 presents the power spectra of axial force F_x, strong axis bending moment M_z, and weak axis bending moment M_y at A6 under EC1 and EC2. These power spectra are based on the average of 100 ensembles. The corresponding contributions from dominant modes to the power spectra are also demonstrated in Fig. 7. It is found that under EC1, variation in the axial force is dominated by wave frequency responses and high-frequency resonant responses, while under EC2, the third-mode resonant response plays a more important role. Regarding the strong axis bending moment, its power spectrum is mainly dominated by wave-frequency responses and high-frequency resonant responses under EC1, but under EC2 it is mainly dominated by the first-mode resonant responses. With

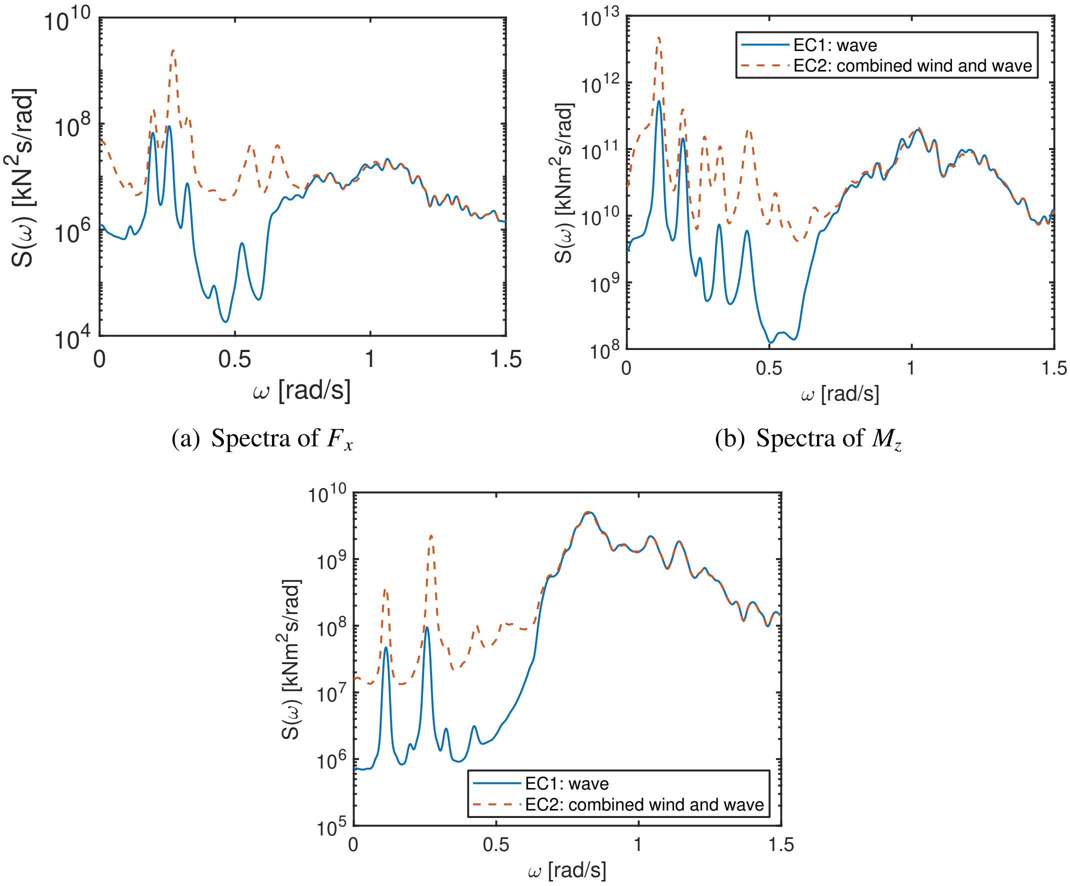

(a) Spectra of F_x

(b) Spectra of M_z

(c) Spectra of M_y

Figure 6: Power spectra of axial force F_x, strong axis bending moment M_z, and weak axis bending moment M_y at A6 under EC1 with wave only and EC2 with combined wind and waves. The power spectra are averaged spectra from 100 ensembles.

respect to the weak axis bending moment, its power spectrum is dominated by wave-frequency responses and high-frequency resonant responses under both EC1 and EC2.

While there are potential non-linearities relating to loads and structural features that make the response non-Gaussian, it is found that the dominance of linear wave frequency loading and the occurrence of resonances make it. This is further analyzed in the next subsection by investigating the statistics of the structural responses.

5.2. Statistics of structural responses

The statistics of structural responses are calculated to show the effect of statistical uncertainty and Gaussianity. The statistical moments for nodes along the bridge girder are calculated for each time series, and then ensemble averaging is conducted. The Gaussian distributed responses are characterized by a skewness of 0 and a kurtosis of 3.

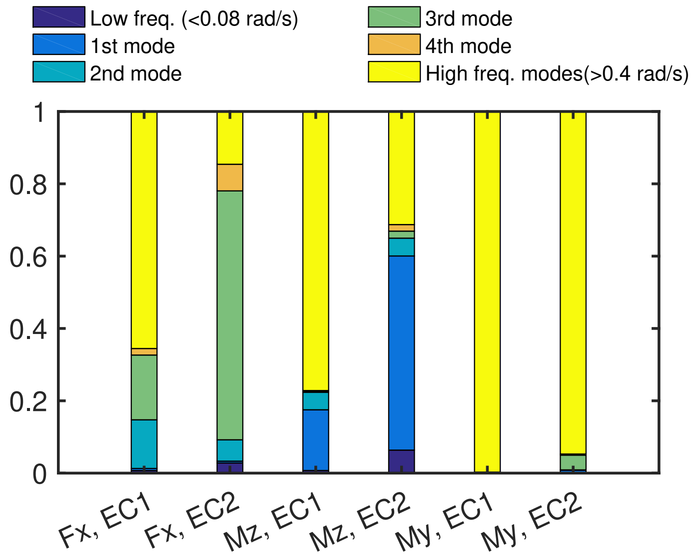

Figure 7: Comparison of power spectra contributions from dominant modes for axial force F_x, strong axis bending moment M_z, and weak axis bending moment M_y at A6 under EC1 with wave only and EC2 with combined wind and waves. The power spectra are averaged spectra from 100 ensembles. The dominant eigen-frequencies are given in Table 3.

Statistical analyses indicate that the skewness of axial force F_x, strong axis bending moment M_z, and weak axis bending moment M_y along the bridge girder is all close to zero, varying mainly within [-0.1, 0.1]. The ensemble average of skewness of F_x, M_z and M_y is also very close to zero. That implies that the distribution of F_x, M_z and M_y is symmetric.

Regarding the kurtosis, F_x, M_z and M_y along the bridge girder in general have a larger variation in kurtosis than in skewness, as shown in Fig. 8. Fig. 8 shows the kurtosis of M_z along the bridge girder. Under EC1 with wave only condition, the kurtosis varies mainly within [2.7, 3.3]. The average kurtosis is almost constant along the bridge girder, close to 3. However, under EC2 with combined wind and wave condition, kurtosis varies within [2.5, 3.5]. The average kurtosis changes along the bridge girder and in general, the average kurtosis is slightly smaller than 3. This implies that the non-Gaussianity in EC2 is slightly stronger than that in EC1. Nevertheless, the non-Gaussianity is generally weak and the stochastic process of structural responses is close to be Gaussian.

In addition, the statistics of structural responses at A6 is presented in details for further analyses. Table 5 gives the ensemble averages of statistical moments of F_x, M_z and M_y of the bridge girder at A6 under EC1 and EC2 based on 100 ensembles. The mean values and standard deviations for different sets of F_x and M_z with different ensemble numbers at A6 are shown in Figs. 9-10. The mean values and standard deviations are normalized by corresponding values with 100 ensembles given in Table 5. It can be found that both the normalized mean value and standard

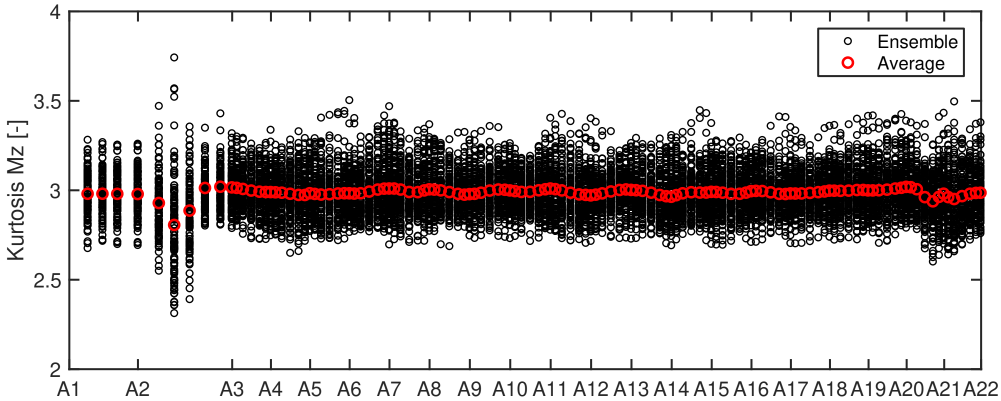

(a) Under EC1 with wave only condition

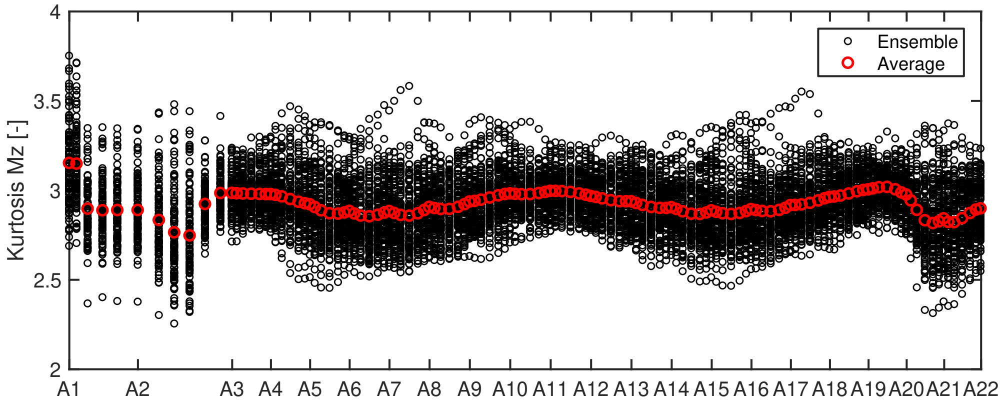

(b) Under EC2 with combined wind and wave condition

Figure 8: Kurtosis of strong axis bending moment M_z along the bridge girder under EC1 with wave only condition and EC2 with combined wind and wave condition. 100 ensemble samples are considered.

deviation have relatively large variation, especially when fewer ensembles (e.g. 10 ensembles) are considered. For instance under EC2, the normalized standard deviation of F_x ranges from 0.94 to 1.05 for different sets of 10 ensembles. Moreover, because of wind-induced load effects, variation in the normalized standard deviation under EC2 is larger than that under EC1.

5.3. Extreme response estimation by a simplified analytical method

Since the structural responses are likely to have a Gaussian distribution, the extreme responses can thus be roughly estimated by the analytical method existing for Gaussian processes, as described in Section 3.2.3. The structural responses of the floating bridge can be simulated by fully coupled time-domain simulations. Accordingly, we can estimate the zero up-crossing period and bandwidth based on the spectral moments. If the structural responses are not wide-banded, the multiplying factor, i.e. for a fractile of 90%, can be approximated according to Fig. 5. It should be noted that this is a simplified approach because it is based on the assumption that the response pro-

Table 5: Ensemble averages of statistical properties of axial force F_x, strong axis bending moment M_z and weak axis bending moment M_y at A6 for the floating bridge under EC1 and EC2 based on 100 ensembles. SD denotes standard deviation.

Response	EC	Average statistics			
		Mean [kN or kN·m]	SD [kN or kN·m]	Skewness	Kurtosis
F_x at A6	EC1	2.69E+02	3.19E+03	-0.01	2.98
	EC2	-1.60E+04	8.55E+03	0.00	2.89
M_z at A6	EC1	3.44E+04	2.47E+05	0.00	2.98
	EC2	1.22E+05	4.26E+05	0.01	2.88
M_y at A6	EC1	-9.04E+05	3.30E+04	0.00	3.00
	EC2	-9.08E+05	3.42E+04	0.00	3.00

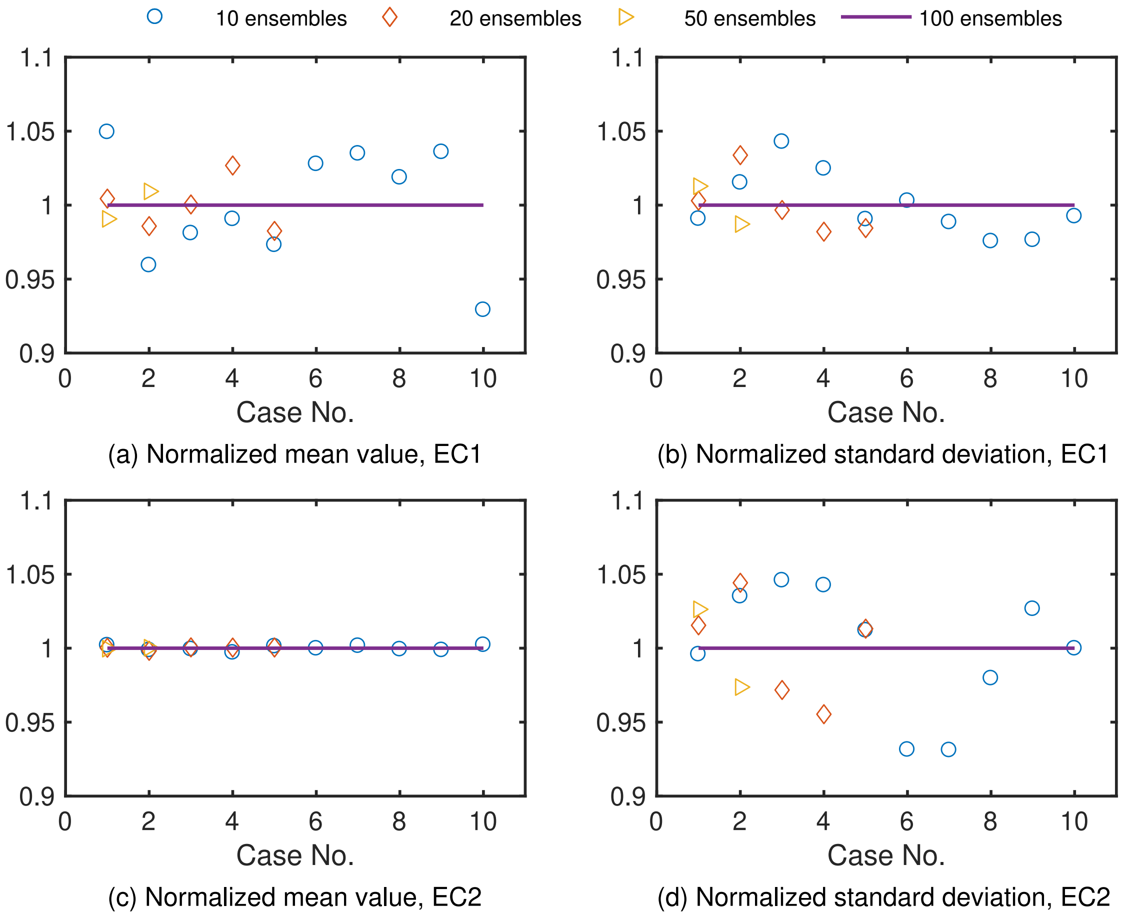

(a) Normalized mean value, EC1

(b) Normalized standard deviation, EC1

(c) Normalized mean value, EC2

(d) Normalized standard deviation, EC2

Figure 9: Normalized mean values and standard deviations of axial force F_x at A6 under EC1 with wave only condition and EC2 with combined wind and wave condition. Various set of ensemble numbers are considered. The values are normalized by corresponding values with 100 ensembles given in Table 5.

cess is Gaussian. The estimated multiplying factor can give a rough estimation of extreme value together with the mean value and standard deviation for the set considered, but a more accurate extreme value is required to be estimated by extrapolation methods.

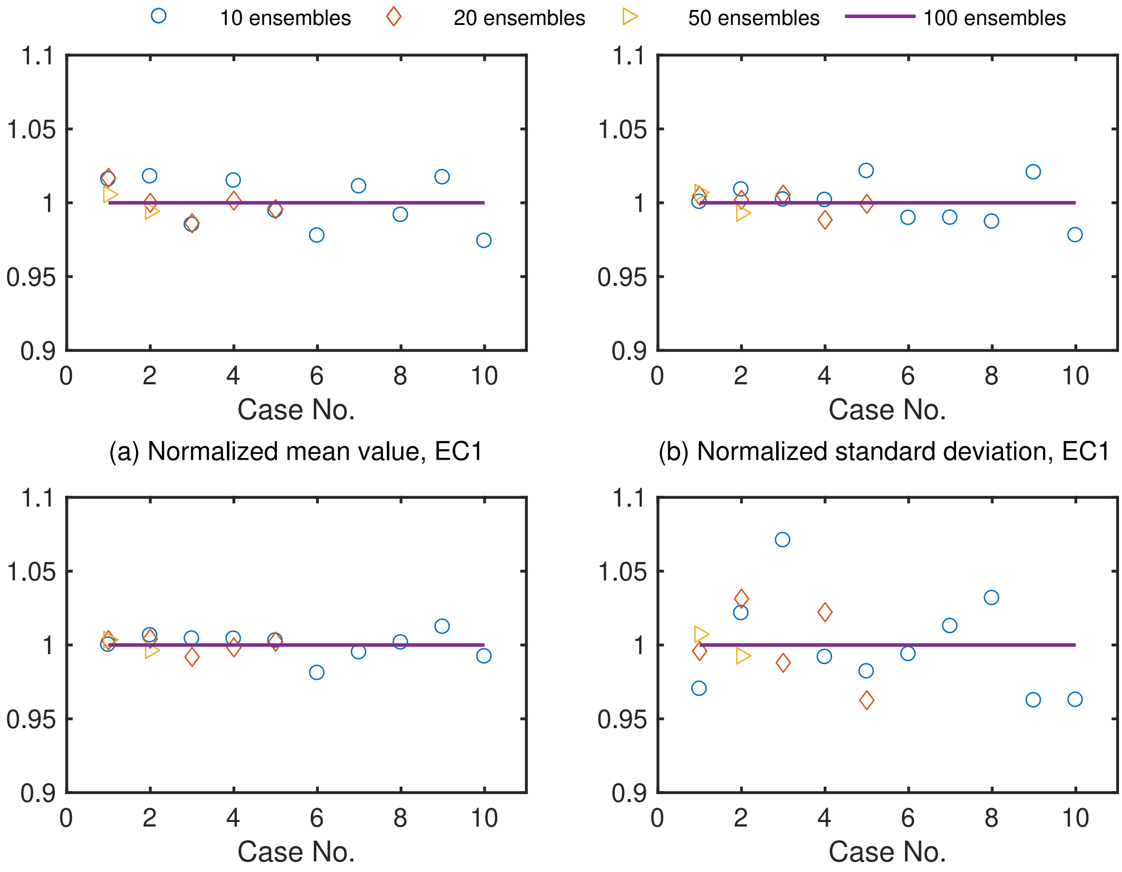

(a) Normalized mean value, EC1

(b) Normalized standard deviation, EC1

(c) Normalized mean value, EC2

(d) Normalized standard deviation, EC2

Figure 10: Normalized mean values and standard deviations of strong axis bending moment M_z at A6 under EC1 with wave only condition and EC2 with combined wind and wave condition. Various set of ensemble numbers are considered. The values are normalized by corresponding values with 100 ensembles given in Table 5.

5.4. Extreme response estimation by extrapolation methods

300 In this section, the extrapolation method is applied to estimate the long-term extreme response that corresponds to a 90% fractile of short-term extreme responses. Both the Gumbel method and the mean upcrossing rate (MUR) method are employed to extrapolate the extreme response at the 90% fractile. The predicted extreme response is denoted as R.

5.4.1. Gumbel method

305 The Gumbel method is first employed. According to Eqs. 3 and 4, the response X is plotted versus $-\log(-\log(F))$ based on N samples. Least square fitting of X as a function of $-\log(-\log(F))$ is then used to determine the parameters of the Gumbel distribution. Knowing the fitted Gumbel distribution, the extreme value R can thus be determined at the 90% fractile level.

The 95% confidence interval (CI) is commonly used to represent the uncertainty associated with the estimated extreme value. The bootstrapping method can be used to evaluate the CI [6]. A large number of bootstrap samples of size N are first randomly generated from the fitted Gumbel distribution. For each sample, a new Gumbel distribution would be fitted and predicts an estimate R^* of R. In the present study, 10000 samples are employed to create the distribution of R^*. The 95% CI of R can be therefore determined from the distribution of R^*.

Two examples are shown in Figs. 11 to demonstrate the extreme value estimation by Gumbel method. The extreme axial force at A6 under EC1 is predicted based on 10 ensembles and 100 ensembles, respectively. It is found that using 100 ensembles leads to an estimated multiplying factor κ of about 4.08 with 95% CI (3.94, 4.24), while using 10 ensembles gives an estimated κ of about 4.14 with 95% CI (3.63, 4.75). Although the estimated κ between the two different ensemble numbers are fairly close, their 95% CIs differ significantly.

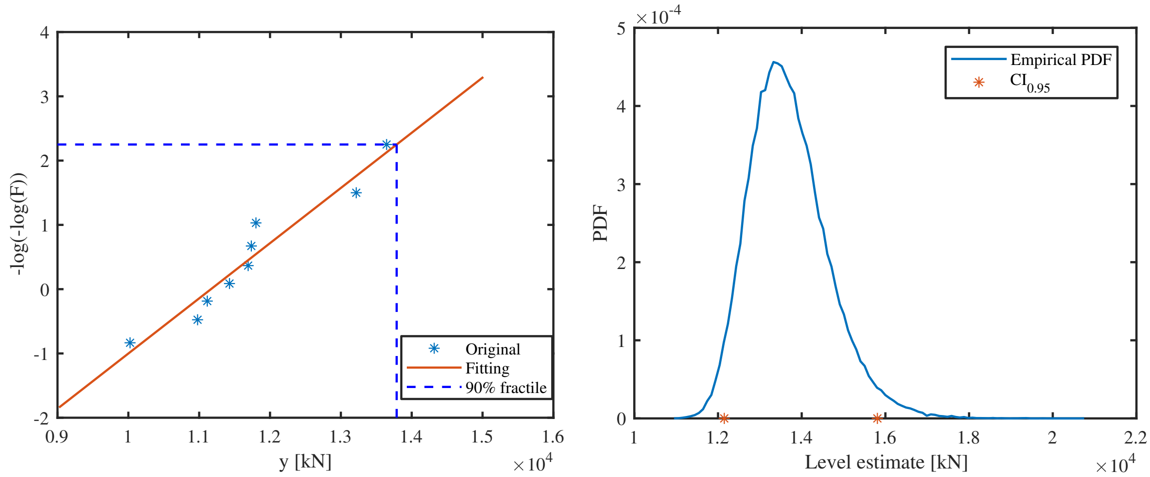

(a) Gumbel fitting (b) Empirical PDF of predicted extreme value

Figure 11: Estimation of extreme axial force at A6 under EC1 based on 10 ensembles by using the Gumbel method. (a) Gumbel fitting of the sample data. (b) empirical PDF of predicted extreme value. Extreme load = $\mu + \kappa\sigma$, μ = 266.67 kN, σ = 3269.77 kN, κ = 4.14 and $\mathrm{CI}^{\kappa}_{0.95} = (3.63, 4.75)$

5.4.2. Mean upcrossing rate method

In the mean upcrossing rate method, the mean upcrossing rate and its 95% CI of a sample of size N are first estimated based on a number of realizations [6]. Extrapolation method by Eq. 6 is then employed to fit the mean upcrossing rate as well as the corresponding 95% CI. According to Eq. 5, the target upcrossing rate level corresponding to 90% fractile in a period of 1 hour is determined to be 2.93×10^{-5}. The extreme value and its 95% CI can thus be determined from fitted mean upcrossing rate and 95% CI at the target upcrossing level.

Fig. 13 is shown as an example of estimation of extreme axial force at A6 under EC1 based on

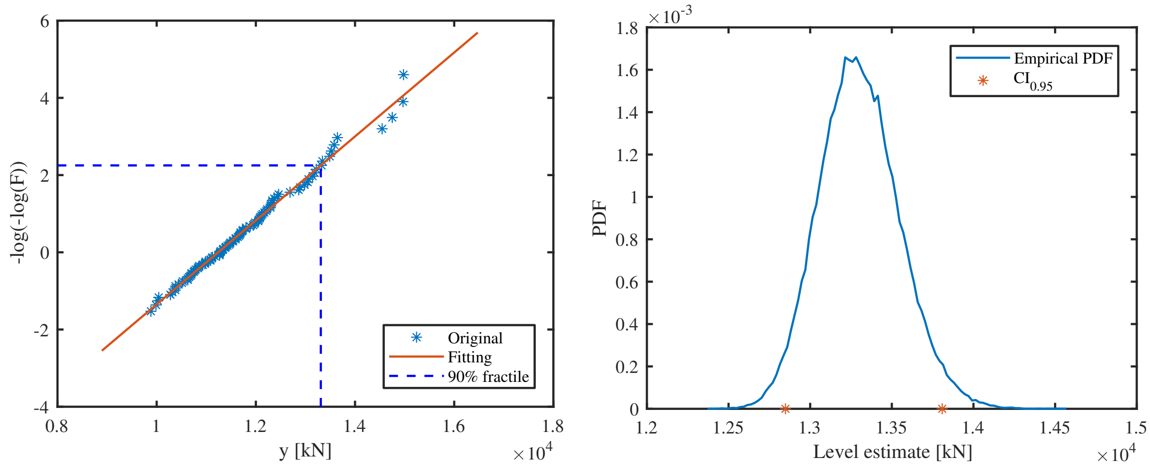

(a) Gumbel fitting (b) Empirical PDF of predicted extreme value

Figure 12: Estimation of extreme axial force at A6 under EC1 based on 100 ensembles by using the Gumbel method. (a) Gumbel fitting of the sample data. (b) empirical PDF of predicted extreme value. Extreme load = $\mu + \kappa\sigma$, μ = 269.24 kN, σ = 3193.83 kN, κ = 4.08 and $CI^{\kappa}_{0.95} = (3.94, 4.24)$

10 ensembles and 100 ensembles. It can be observed that the estimated factor κ for 100 ensembles is about 4.08 with a 95% CI (3.92, 4.21). For 10 ensembles, the estimated factor κ is about 4.08 with a 95% CI (3.75, 4.36).

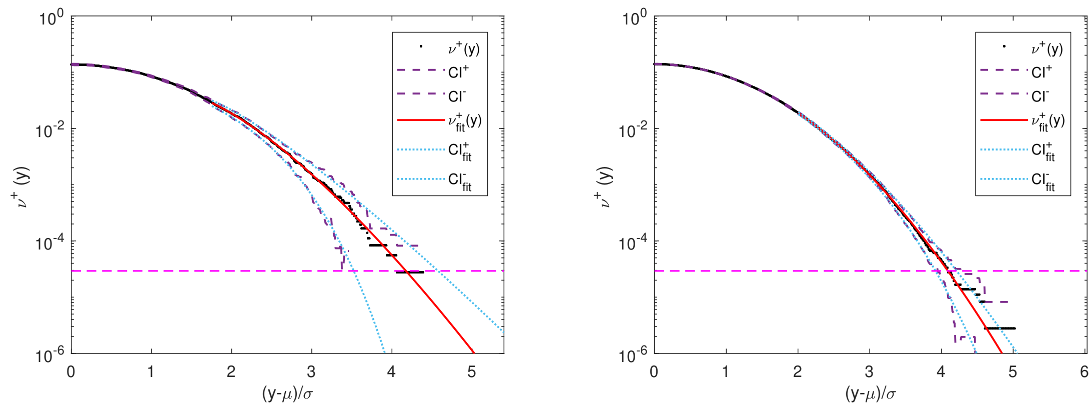

(a) Based on 10 ensembles (b) Based on 100 ensembles

Figure 13: The mean upcrossing rate of axial force at A6 under EC1. CI denotes the empirical 95% confidence interval. (a) based on 10 ensembles. Extreme load = $\mu + \kappa\sigma$, , μ = 268.01kN, σ = 3293.6kN, κ = 4.08 and $CI^{\kappa}_{0.95} = (3.75, 4.36)$ (b) based on 100 ensembles. Extreme load = $\mu + \kappa\sigma$, μ = 268.92kN, σ = 3194.6kN, κ = 4.08 and $CI^{\kappa}_{0.95} = (3.92, 4.21)$

5.5. Multiplying Factor

5.5.1. Simplified method vs. extrapolation method

In this section, the simplified method is verified by comparison the multiplying factor κ to that estimated by the Gumbel method. Table 6 compares the multiplying factor of axial force F_x, strong axis bending moment M_z and weak axis bending moment M_y of the bridge girder at A6, A11, and A15 estimated by these two methods. For the simplified method, the zero up-crossing periods and bandwidth parameters are calculated based on the averages spectra of 100 ensembles. The same ensembles are also considered for the Gumbel method.

For all responses considered, the skewness is almost zero. Most responses are associated with a kurtosis of very close to 3, while four responses have a kurtosis of about 2.9. The bandwidth parameter mainly ranges from 0.8 to 0.92; however, several responses have a bandwidth parameter larger than 0.96, which implies that these responses are extremely narrow-banded.

In general, the simplified method gives an overall good prediction of multiplying factor compared to the Gumbel method, as the difference is within 4%. Relatively large discrepancy is likely to occur if the kurtosis deviates a lot from 3 or if the bandwidth parameter is too close to one (i.e. the responses are too narrow-banded). Although Eq. 10 is employed to account for the effect of bandwidth, the discrepancy is still slightly large for extremely narrow-banded responses.

5.5.2. Gumbel method vs. mean upcrossing rate method

The two extrapolation methods, i.e. the Gumbel method and MUR method, are compared in this section for estimation of the factor κ. As mentioned above, the total 100 ensemble is grouped into 2 sets with 50 ensembles, 5 sets with 20 ensembles and 10 sets with 10 ensembles, respectively. For each set, the Gumbel method and MUR method are applied to estimate the multiplying factor.

Fig. 14 presents the estimated multiplying factor κ of axial force F_x of the bridge girder at A6, A11 and A15 under EC1 with wave only condition and under EC2 with combined wind and wave condition. The factor κ for each response is the average value for different sets with identical ensemble number. The κ estimated by the Gumbel method and the MUR method are generally close, with slight discrepancies. Comparing the κ of F_x of the bridge girder at A6, A11 and A15 estimated based on 100 ensembles indicates that the MUR method gives slightly larger prediction of κ than the Gumbel method. For the Gumbel method, the set-averaged values of κ of F_x are fairly close among different ensemble numbers. However, these set-averaged values of κ estimated by the MUR method exhibit differences, especially for F_x at A15 under EC1, F_x at A6 under EC2. Similar trends are also observed for the strong axis bending moment M_z of the bridge girder at A6, A11 and A15.

Table 6: Comparison of multiplying factor κ of axial force F_x, strong axis bending moment M_z and weak axis bending moment M_y of the bridge girder at A6, A11, and A15 estimated by the simplified method and Gumbel method based on 100 ensembles. SAM denotes the simplified analytical method.

Location	EC	Response	Skewness	Kurtosis	T_z	α_b	κ		Diff [%]
							SAM	Gumbel	
A6	EC1	F_x	-0.01	2.98	7.15	0.87	4.11	4.08	0.75
		M_z	0.00	2.98	6.45	0.89	4.14	4.14	-0.06
		M_y	0.00	3.00	6.36	0.97	4.10	4.23	-2.97
	EC2	F_x	0.00	2.89	14.38	0.80	3.94	3.81	3.47
		M_z	0.01	2.88	10.68	0.67	4.02	4.10	-1.92
		M_y	0.00	3.00	6.57	0.96	4.11	4.22	-2.49
A11	EC1	F_x	-0.01	2.97	8.00	0.84	4.09	4.16	-1.69
		M_z	0.00	3.01	6.42	0.94	4.13	4.13	0.00
		M_y	0.00	3.00	6.92	0.97	4.08	4.13	-1.22
	EC2	F_x	-0.01	2.90	15.84	0.83	3.92	3.81	2.91
		M_z	0.00	2.99	7.77	0.85	4.09	4.10	-0.19
		M_y	0.00	2.99	7.01	0.97	4.09	4.12	-0.88
A15	EC1	F_x	-0.01	2.98	6.69	0.90	4.13	3.97	3.86
		M_z	0.01	2.99	6.58	0.91	4.13	4.06	1.75
		M_y	0.00	3.02	6.38	0.97	4.11	4.24	-3.14
	EC2	F_x	-0.01	2.94	12.73	0.80	3.97	3.94	0.93
		M_z	0.02	2.89	10.56	0.69	4.02	3.92	2.63
		M_y	0.00	3.01	6.46	0.96	4.11	4.16	-1.23

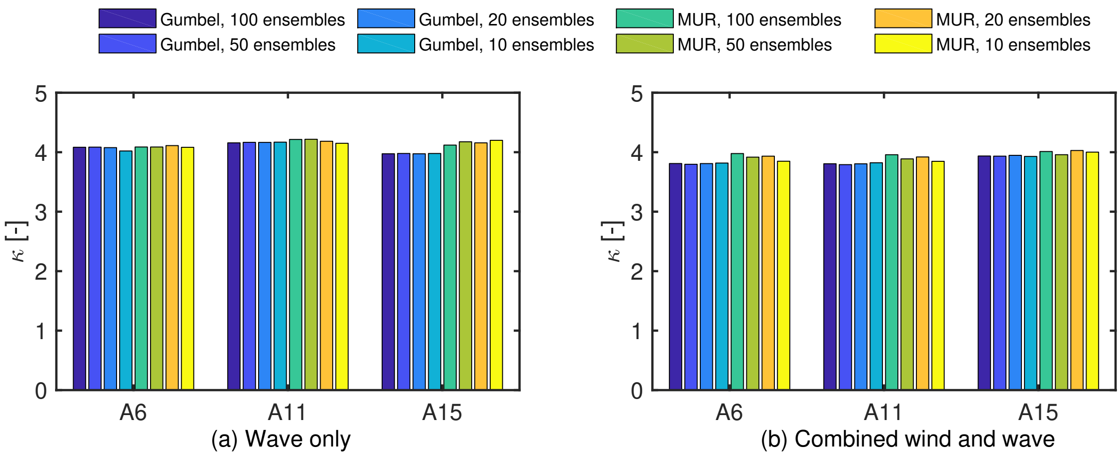

Figure 14: Comparison of estimated multiplying factor κ for axial force at A6, A11 and A15 by using Gumbel method and MUR method. κ is the averaged value for sets with identical ensemble number. Extreme load = $\mu + \kappa\sigma$.

It should be noted that the factor κ presented in Fig. 14 is the average value for sets with identical ensemble number. Variation of κ among different sets with identical ensemble number is addressed in the next section.

6. Uncertainty in extreme response estimation

Uncertainty always exists in the prediction of extreme structural responses for offshore structures. The main sources of uncertainties are related to the accuracy of simulated structural responses, the approach used for prediction of extreme response, and a limited number of numerical simulations, etc.

The uncertainties addressed in this section mainly focus on the statistical uncertainties due to a limited number of simulations and related to the predicted statistical parameters, and the model uncertainties related to approach for extreme response prediction.

6.1. Statistical uncertainty

In the estimation of extreme responses for a complex structural system like a very-long floating bridge, each simulation is usually very time-consuming. Therefore, the extreme responses are desirable to be determined based on a limited number of simulations. This will, unavoidably, introduce statistical uncertainties. Besides, in this study, the extreme response is expressed by $X_{max} = \mu + \kappa \cdot \sigma$, as given by Eq 1. Statistical uncertainties also exist in the prediction of these statistical parameters. Both these statistical uncertainties are addressed here. Uncertainties in the predicted parameters of μ, σ and κ are discussed first.

6.1.1. Uncertainty related to predicted statistical parameters.

The mean value μ and standard deviation σ are both likely to be affected by the number of simulations. This has been demonstrated in Figs. 9 and 10. As the number of simulation increases, the uncertainties in μ and σ decreases. The mean and coefficients of variation (CoV) of the μ and σ of the axial force F_x and strong axis bending moment M_z of the bridge girder at A6 and A11 are given in Table 7, based on 10 sets of 10 ensembles. Here the CoV is defined as the ratio of standard deviation and mean value. Relatively large CoV values are observed in both μ and σ.

The factor κ is estimated by using both the simplified analytical method and extrapolation methods in the present study. The effect of a limited number of simulations on the prediction of κ by using the simplified analytical method is first addressed. The simplified method determines the κ value based on the calculated zero up-crossing period and bandwidth parameter from spectral moments. Therefore, the simplified method can predict an estimation of the factor κ even given only one ensemble. In Table 7, the factor κ is estimated based on 10 sets of 10 ensembles. For axial force F_x and strong axis bending moment M_z of the bridge girder at A6 and A11, the CoV of κ estimated are all very small, less than 0.002. This is because small variations in zero up-crossing period or bandwidth parameter (less than 0.9) do not cause large variation in the estimated κ

Table 7: Mean value and coefficient of variation (CoV) of mean value μ, standard deviation σ, factor κ and extremes of the axial force F_x, strong axis bending moment M_z of the bridge girder at A6 and A11.Among them, mean of μ, σ, κ, extreme value $X_{max,10}$ and their CoVs are calculated based on 10 sets of 10 ensembles. The mean extreme value $X'_{max,10}$ is calculated by $X'_{max} = \mu + \kappa \cdot \sigma$. The CoV of $X'_{max,10}$ is calculated according to Eq. 14. The mean extreme value $X_{max,100}$ is calculated based on 100 ensembles. SAM denotes the simplified analytical method.

Location	EC	Response	Method	Statistics calculated from 10 sets of 10 ensembles								Derived statistics		100 ensemles
				μ		σ		κ		$X_{max,10}$		$X'_{max,10}$		$X_{max,100}$
				Mean	CoV	Mean	CoV	Mean	CoV	Mean	CoV	Mean	CoV	Mean
				kN or kNm		kN or kNm				kN or kNm		kN or kNm		kN or kNm
A6	EC1	F_x	Gumbel	2.69E+02	0.039	3.19E+03	0.022	4.020	0.059	1.31E+04	0.065	1.31E+04	0.062	1.33E+04
			MUR	2.69E+02	0.039	3.19E+03	0.022	4.082	0.027	1.33E+04	0.033	1.33E+04	0.034	1.33E+04
			SAM	2.69E+02	0.039	3.19E+03	0.022	4.114	0.001	1.34E+04	0.020	1.34E+04	0.021	1.34E+04
		M_z	Gumbel	3.44E+04	0.017	2.47E+05	0.014	4.116	0.048	1.05E+06	0.043	1.05E+06	0.049	1.06E+06
			MUR	3.44E+04	0.017	2.47E+05	0.014	4.187	0.055	1.07E+06	0.058	1.07E+06	0.055	1.06E+06
			SAM	3.44E+04	0.017	2.47E+05	0.014	4.137	0.001	1.06E+06	0.014	1.06E+06	0.014	1.06E+06
	EC2	F_x	Gumbel	-1.60E+04	-0.002	8.55E+03	0.042	3.818	0.020	1.67E+04	0.095	1.67E+04	0.091	1.66E+04
			MUR	-1.60E+04	-0.002	8.55E+03	0.042	3.848	0.052	1.70E+04	0.145	1.69E+04	0.130	1.80E+04
			SAM	-1.60E+04	-0.002	8.55E+03	0.042	3.942	0.002	1.77E+04	0.078	1.77E+04	0.080	1.77E+04
		M_z	Gumbel	1.22E+05	0.009	4.26E+05	0.035	4.029	0.063	1.84E+06	0.081	1.84E+06	0.067	1.87E+06
			MUR	1.22E+05	0.009	4.26E+05	0.035	4.106	0.049	1.87E+06	0.056	1.87E+06	0.056	1.88E+06
			SAM	1.22E+05	0.009	4.26E+05	0.035	4.018	0.002	1.83E+06	0.031	1.83E+06	0.032	1.83E+06
A11	EC1	F_x	Gumbel	-6.93E+02	-0.015	2.74E+03	0.029	4.169	0.055	1.07E+04	0.066	1.07E+04	0.066	1.07E+04
			MUR	-6.93E+02	-0.015	2.74E+03	0.029	4.150	0.044	1.07E+04	0.056	1.07E+04	0.056	1.09E+04
			SAM	-6.93E+02	-0.015	2.74E+03	0.029	4.087	0.001	1.05E+04	0.031	1.05E+04	0.031	1.05E+04
		M_z	Gumbel	1.08E+05	0.003	2.48E+05	0.012	4.046	0.045	1.11E+06	0.042	1.11E+06	0.042	1.13E+06
			MUR	1.08E+05	0.003	2.48E+05	0.012	4.247	0.034	1.16E+06	0.033	1.16E+06	0.033	1.13E+06
			SAM	1.08E+05	0.003	2.48E+05	0.012	4.127	0.000	1.13E+06	0.011	1.13E+06	0.011	1.13E+06
	EC2	F_x	Gumbel	-1.70E+04	-0.002	8.35E+03	0.043	3.822	0.048	1.50E+04	0.137	1.50E+04	0.137	1.48E+04
			MUR	-1.70E+04	-0.002	8.35E+03	0.043	3.847	0.061	1.52E+04	0.158	1.52E+04	0.158	1.61E+04
			SAM	-1.70E+04	-0.002	8.35E+03	0.043	3.917	0.002	1.57E+04	0.088	1.57E+04	0.088	1.57E+04
		M_z	Gumbel	1.48E+05	0.007	3.18E+05	0.012	4.114	0.054	1.45E+06	0.050	1.45E+06	0.050	1.45E+06
			MUR	1.48E+05	0.007	3.18E+05	0.012	4.229	0.032	1.49E+06	0.031	1.49E+06	0.031	1.46E+06
			SAM	1.48E+05	0.007	3.18E+05	0.012	4.094	0.000	1.45E+06	0.011	1.45E+06	0.011	1.45E+06

value. This implies that with respect to the simplified analytical method, few ensemble can give a reasonably good estimation of the factor κ. The estimation of the factor κ by using the simplified analytical method is not sensitive to the number of simulations.

In terms of extrapolation methods (e.g. the Gumbel method), since the ensemble number can affect the determination of fitting parameters involved in the extrapolation models, this will of course cause statistical uncertainty, especially when the ensemble number is limited. In general, the larger the ensemble number, the smaller the uncertainties. These uncertainties are often expressed as 95% confidence interval (CI) of the predicted extreme value. Approaches on estimation of 95% CI of extreme value by Gumbel method and MUR method have been elaborated in the previous sections. Comparing Fig. 11 and Fig. 12 indicates that the κ of F_x of the bridge girder at A6 estimated by the Gumbel method based on 100 ensembles has a significantly smaller range of

95% CI, i.e., $CI_+ - CI_-$, than that based on 10 ensembles. 10 ensembles gives a 95% CI range of about 1.12, which is approximately 3.7 times of the value from 100 ensembles. Similar conclusions is also drawn from Fig. 13. Therefore, large uncertainty may exist when only 10 ensembles are used to predicted the extreme response.

Moreover, when the extrapolation methods are employed, statistical uncertainties also exist for a fixed ensemble number, due to the selection of random ensembles. Fig. 14 shows the set-averaged multiplying factor κ of axial force F_x for different ensemble number, which are more or less close for both the Gumbel method and the MUR method. However, for a fixed ensemble number, the estimated κ has great variation, in particular only 10 ensembles are used for extreme value estimation. This is clearly illustrated in Figs. 15 and 16.

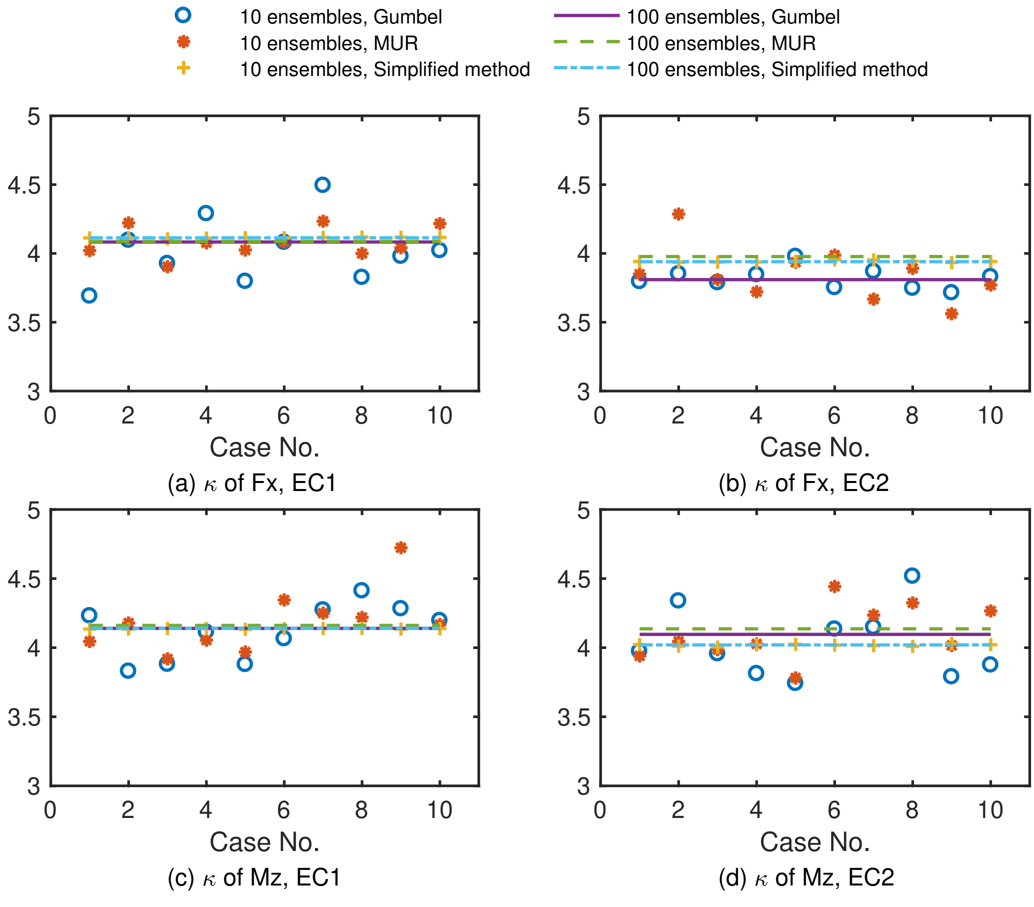

Figure 15: Comparison of estimated multiplying factor κ for axial force and strong axis bending moment at A6 by using the Gumbel method, the MUR method and the simplified analytical method. Two sets of ensemble numbers are considered.

Figs. 15 and 16 demonstrate the variation in the estimated multiplying factor κ of F_x and M_z of the bridge girder at A6 and A11, respectively. Two sets of ensembles, i.e. with 10 ensembles and

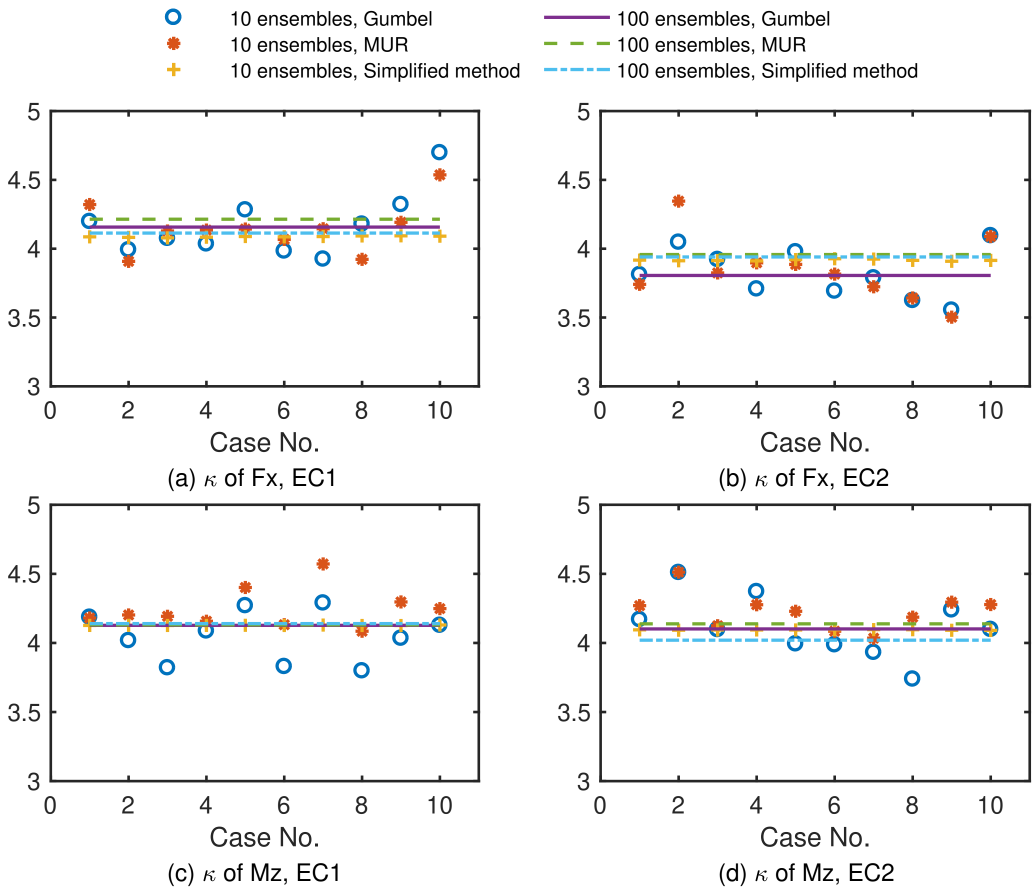

Figure 16: Comparison of estimated multiplying factor κ for axial force and strong axis bending moment at A11 by using the Gumbel method, the MUR method and the simplified analytical method. Two sets of ensemble numbers are considered.

100 ensembles, are considered for both EC1 with wave only condition and EC2 with combined wind and wave condition. It can be found that as the ensemble number increases, variations in the κ decrease. Both the κ estimated by the Gumbel method and by the MUR method has great variations when 10 ensembles are used for extreme value prediction. For instance, κ of F_x under EC1 estimated by the Gumbel method has a largest value of 4.50 and a smallest value of about 3.69 based on 10 ensembles, while the corresponding value κ based on 100 ensembles is about 4.08. This implies that the deviations might be as large as approximately 10%.

6.1.2. Uncertainty in predicted extreme values caused by statistical parameters.

Based on the above discussions, uncertainties exist in the prediction of mean value μ, the standard deviation σ and the factor κ. Such uncertainties will affect the evaluation of extreme responses, resulting in uncertainties. Since the standard deviation σ and the factor κ are usually statistically independent, the CoV of the extremes $X_{max} = \mu + \kappa \cdot \sigma$ caused by CoVs in μ, σ, κ can be estimated by

$$CoV_{X_{max}} = \frac{|\sigma \cdot \kappa|}{\mu + \sigma \cdot \kappa} \sqrt{(\frac{\mu}{\sigma \cdot \kappa})^2 \cdot CoV_\mu^2 + CoV_\kappa^2 + CoV_\sigma^2} \tag{14}$$

The derivation of Eq. 14 is given in the Appendix. It is found that when the absolute value of mean μ is smaller than the standard deviation σ, e.g. for the axial force F_x, strong axis bending moment M_z of the bridge girder, the CoV of X_{max} is mainly affected by the CoV of σ and κ. However, when the absolute value of mean μ is much larger than σ, e.g. for the weak axis bending moment M_y of the bridge girder, the CoV of μ will also make a contribution to the CoV of X_{max}, but the CoV of X_{max} is expected to be small.

The uncertainty in the calculated X_{max} is demonstrated by considering 10 sets of 10 ensembles. The mean value and CoV of μ, κ, σ, X_{max} and of the axial force F_x, strong axis bending moment M_z of the bridge girder at A6 and A11 are estimated by using the simplified analytical method and two extrapolation methods, as given in Table 7. It can be observed that the extreme value X_{max} has a greater value of CoV than the μ, κ and σ. The CoV of X_{max} estimated by the Gumbel and MUR methods are higher than that by the simplified analytical method. This is because the simplified analytical method uses the m^i spectral moments based on large amount of data, while the MUR method uses the tail distribution based on limited amount of data. The CoV of X_{max} by the simplified analytical method is less than 0.035, while the CoV of X_{max} estimated by the Gumbel and MUR methods can reach 0.137 and 0.158, respectively.

The extreme values are also estimated by $X'_{max} = \mu + \kappa \cdot \sigma$ based on the mean values of μ, κ and σ. The standard error of X'_{max} are calculated by Eq. 14; accordingly, the CoV of X'_{max} is estimated and given in Table 7. Comparison between X_{max} and X'_{max} indicates that their values are fairly close for the response and EC considered. So do their CoVs. This implies that Eq. 14 can give a reliable prediction of standard error of the extreme value. In addition, the CoV of X_{max} estimated by the three methods are strongly affected by the relative values of mean value μ and standard deviation σ. When the simplified analytical method is used, the CoV of X_{max} is mainly affected by the CoV of σ when the standard deviation σ is larger than the mean value μ. When the standard deviation σ is more than two times larger than the absolute value of mean μ, the CoV of X_{max} estimated by the Gumbel and MUR method are both smaller than 0.07 for the cases considered in Table 7. However, when the standard deviation σ is smaller than the absolute value of mean μ, extremely large CoV of X_{max} are observed, for instance the axial force F_x at A6 and A11 under EC2. It gives the CoV of X_{max} of about 0.158 for the MUR method and 0.137 for the Gumbel method.

The extreme values estimated by 100 ensembles based on the three approaches are also given in Table 7. Comparing the extremes predicted by 100 ensembles and 10 ensembles shows that the averaged extremes by 10 sets of 10 ensembles generally agrees well with the extremes by

100 ensembles, except that the MUR method might underestimates or overestimates the extremes under some cases.

6.1.3. Uncertainty in predicted extreme value due to a limited number of simulations

The accuracy of predicted extreme values due to a limited number of simulations is addressed in this section. Assuming M sets of time domain simulations are carried out to predict the extreme responses, the predicted extremes are denoted by $X_{max,i}, i = 1, 2, ..., M$, in which $X_{max,i}$ are considered to be statistically independent. The final estimate of this extreme is considered as the ensemble average of these extremes. The error in the extreme estimate is a random variable. It has a zero mean and the root mean square error of the extreme estimate is given by [31]

$$\delta = \frac{1}{\sqrt{M}} \frac{\sigma_{X_{max}}}{\mu_{X_{max}}} \tag{15}$$

where $\mu_{X_{max}}$ and $\sigma_{X_{max}}$ are the exact mean value and standard deviation of the extreme. The derivation of Eq. 15 is given in the Appendix.

The error in the extreme estimate follows a Gaussian distribution with zero mean and a standard deviation of $\frac{\sigma_{X_{max}}}{\sqrt{M}}$. To achieve a 90% conservative estimate of the extreme due to M sets of simulations, a correction factor should be multiplied with the extreme estimate, i.e.

$$\mu_{X_{max}} \cdot \gamma \geq \mu_{X_{max}} + 1.28 \frac{\sigma_{X_{max}}}{\sqrt{M}} \tag{16}$$

This gives

$$\gamma \geq 1 + 1.28 \frac{CoV_{X_{max}}}{\sqrt{M}} \tag{17}$$

where $CoV_{X_{max}}$ is the exact CoV of the extreme.

In the practical design of floating bridges, if only one set of 10 1-h simulations is used and simulated to predict the extreme structural responses. Assuming that the exact CoV of the extreme is approximated by the values estimated in the present study based on 10 sets of 10 1-h simulations, as given in Table 7, it can be found that a correction factor of 1.1 should be used when the responses have a standard deviation larger than its absolute mean value, and a correction factor of 1.2 should be used when the responses have a standard deviation smaller than its absolute mean value.

6.2. Model uncertainty

In this study, the extreme response or the multiplying factor κ is estimated by three different approaches, i.e. the simplified method, the Gumbel method and the MUR method. As given in Tables 6 and 7 and in Figs. 14, 15 and 16, these three methods give different predictions of the multiplying factor κ for structural responses at different locations and under EC1 and EC2. This implies that model uncertainty exist due to extreme value prediction method used.

To evaluate this model uncertainty, the extreme values estimated by the three approaches are analyzed and compared against the reference extremes. The reference extremes are taken as the 90% fractile extreme values from the raw data of the 100 ensembles, and are thus independent of the method used. The results are given in Table 8. Extreme values calculated based on 10 sets of 10 ensembles and based on 100 ensembles by using these three approaches are compared and relative errors are calculated.

Relatively large error are observed in axial force F_x under EC2 at A6 and A11, in which the absolute mean value is significantly larger than the standard deviation. The relative error can reach about 10% for the MUR method and 8% for the simplified analytical method. The Gumbel method gives a better prediction of extremes than the MUR and simplified analytical method under this scenario. When the absolute mean value of the response considered is smaller than the standard deviation, the relative errors predicted by the three methods are generally small, less than 2.5%.

Among these three methods, the κ value and extremes determined by the simplified analytical method is not sensitive to the ensemble number. This is an prominent advantage of the simplified method, compared to the Gumbel method and MUR method that are both sensitive ensemble numbers. However, the accuracy of the simplified method is strongly affected by the Gaussian distribution assumption, as well as the bandwidth parameter if the responses are extremely narrow-banded.

6.3. Recommendation for engineering design

A very-long floating bridge is a very complex structure. During the design of floating bridges, characteristic values of long-term extreme responses are required for ULS design check. Prediction of long-term extreme responses requires tremendous time and effort. Properly reducing the computational time and effort is desirable from engineering design point of view.

The simplified engineering approach based on the environmental contour method, as used in the present study, is an efficient method to reduce the computational effort. In this approach, the long-term extreme responses are approximated by relevant short-term extreme responses at a high fractile.

The computational effort for prediction of short-term extreme responses can be further reduced by using a simplified analytical approach when the structural responses are close to have a Gaussian distribution. This is demonstrated in the present study of a long end-arched floating bridge. As a matter of fact, the long floating bridges commonly feature a large number of eigen-modes. Under the action of wind and waves, the structural responses are dominated by resonant responses at several eigen-modes. Consequently, the structural responses are likely to have a Gaussian dis-

Table 8: Comparison of extremes of the axial force F_x, strong axis bending moment M_z of the bridge girder at A6 and A11 estimated by the three method. Among them, the mean extreme value $X_{max,10}$ are calculated based on 10 sets of 10 ensembles. The mean extreme value $X_{max,100}$ is calculated based on 100 ensembles. SAM denotes the simplified analytical method. The 90% fractile extreme value from the raw data based on 100 ensembles are taken as the characteristic value and used as the reference here.

Location	EC	Response	$X_{max,ref}$	Method	$X_{max,10}$		$X_{max,100}$	
					Mean	Relative error	Mean	Relative error
			kN or kNm		kN or kNm		kN or kNm	
A6	EC1	Fx	1.33E+04	Gumbel	1.31E+04	-1.60%	1.33E+04	-0.11%
				MUR	1.33E+04	0.00%	1.33E+04	0.07%
				SAM	1.34E+04	0.62%	1.34E+04	0.62%
		Mz	1.04E+06	Gumbel	1.05E+06	0.69%	1.06E+06	1.27%
				MUR	1.07E+06	2.48%	1.06E+06	1.84%
				SAM	1.06E+06	1.21%	1.06E+06	1.21%
	EC2	Fx	1.64E+04	Gumbel	1.67E+04	1.59%	1.66E+04	1.16%
				MUR	1.70E+04	3.91%	1.80E+04	10.07%
				SAM	1.77E+04	8.06%	1.77E+04	8.06%
		Mz	1.84E+06	Gumbel	1.84E+06	-0.25%	1.87E+06	1.21%
				MUR	1.87E+06	1.53%	1.88E+06	2.09%
				SAM	1.83E+06	-0.61%	1.83E+06	-0.61%
A11	EC1	Fx	1.06E+04	Gumbel	1.07E+04	1.05%	1.07E+04	0.74%
				MUR	1.07E+04	0.56%	1.09E+04	2.28%
				SAM	1.05E+04	-1.07%	1.05E+04	-1.07%
		Mz	1.12E+06	Gumbel	1.11E+06	-0.68%	1.13E+06	1.12%
				MUR	1.16E+06	3.76%	1.13E+06	1.20%
				SAM	1.13E+06	1.12%	1.13E+06	1.12%
	EC2	Fx	1.53E+04	Gumbel	1.50E+04	-1.90%	1.48E+04	-2.81%
				MUR	1.52E+04	-0.56%	1.61E+04	5.67%
				SAM	1.57E+04	3.27%	1.57E+04	3.25%
		Mz	1.45E+06	Gumbel	1.45E+06	0.23%	1.45E+06	-0.04%
				MUR	1.49E+06	2.75%	1.46E+06	0.75%
				SAM	1.45E+06	-0.21%	1.45E+06	-0.21%

tribution. In the practical design of floating bridges, the Gaussianity of structural responses can be evaluated by assessing the skewness and kurtosis. The simplified analytical method is very efficient and recommended if structural responses are close to have a Gaussian distribution. Otherwise, the Gumbel or MUR methods are more suitable.

Besides, during the evaluation of short-term extreme responses, a limited number of simulations is usually conducted, which will result in statistical uncertainty in the extreme estimate. A correction factor should be used and multiplied with the extreme estimate in order to have a conservative prediction when a limited sample is used. A simplified procedure to derive the correction factor is given in this study. Based on the present study, the extreme structural response can be expressed by $X_{max} = \mu + \kappa \cdot \sigma$, in which the μ, κ and σ are found to be statistically independent. The mean and CoV of μ, κ, σ and extremes are evaluated by considering 10 sets of 10 1-h simulations. If only 10 1-h simulations is used for extreme response prediction in the practical design of floating bridges considered, a correction factor 1.1-1.2 is recommended in order to achieve a 90% conservative estimation of extreme. A correction factor of 1.1 should be used when the responses have a standard deviation larger than its absolute mean value, and a correction factor of 1.2 should be used when the responses have a standard deviation smaller than its absolute mean value. It should be noted that these correction factors are a proposal that could be further scrutinized, since they are derived based on numerical simulations for the present case study.

7. Discussion

This study addresses the determination of the extreme response in short-term periods in the context of long-term extreme structural responses of a very-long floating bridge by using the environmental contour method. The relevant short-term extreme value is defined by a high fractile value. The short-term condition should be properly selected to be the most severe sea state that cause the largest extreme responses. This approach is an engineering approach that has been widely used in the design of marine structures. Although the present floating bridge is a very-long complex infrastructure with a large number of eigen-modes that differs from traditional marine structures, the environmental contour method is still expected to be applicable. However, the contour method is approximate and should be verified by comparison with full long-term method.

The short-term environmental conditions used in this study, i.e., EC1 and EC2 given in Table 4, are determined according to the metocean design basis for the fjord [27]. EC1 is the 100-year worst wave condition. Nevertheless, EC2 is a combination of 100-year worst wind condition and 100-year worst wave condition and we assume that EC2 is the worst combined wind and wave condition with a return period of 100 years. The wave conditions in the fjord considered is mainly wind-generated and also affected by limited fetch length [28]. According to Tucker and Pitt [32], the significant wave height for fetch-limited seas in deep water is given by

$$H_s = 0.0163\sqrt{L_f}U_w \tag{18}$$

where L_f is the fetch length in km. The calculated fetch length corresponding to EC2 is about 24.9km, which is reasonable according to the local topology of the Bjørnafjord. This also implies that the combination of 100-year wind and 100-year wave in EC2 is a reasonable approximation of the worst wind and wave conditions.

A 90% fractile is used in the present study to determine the extreme value. This fractile level is recommended by metocean design basis [27]. It was proposed according to previous experience in the offshore oil and gas industry. However, an accurate fractile value should be calibrated and determined by carrying out a full or simplified long-term analysis.

This study addresses uncertainties related to prediction of extreme responses, mainly statistical uncertainties due to a limited number of simulations and model uncertainties due to approaches for extreme value prediction. However, several other sources of uncertainty also exist, e.g. in environmental conditions, environmental load calculation and load effect estimation, etc.

The environmental conditions (EC1, EC2) are derived based on long-term simulated wind and wave data. These data are not completely validated due to limited field measured data [28]. The wind and wave conditions are assumed to be homogeneous over the whole floating bridge; however, the wind and wave conditions in the fjord are actually inhomogeneous due to complex topology and hydrology [33]. Therefore, uncertainties are unavoidably introduced in the environmental conditions. In the calculation of environmental loads, several simplifications are employed, which of course cause uncertainties. For instance, hydrodynamic interactions between pontoons were ignored, the viscous drag forces on the pontoons were simulated by empirical drag coefficients, and the aerodynamic loads on the bridge girder was modeled by using the nonlinear quasi-static airfoil theory, in which the frequency-dependent aerodynamic force induced by motion of the structures was neglected. The environmental load effects are estimated by using fully coupled numerical models, which might introduce uncertainties as well.

Uncertainty might exist in the fractile level and the determination of short-term environmental conditions that cause the largest extreme responses. The present study assumes that EC2 is likely to cause the most severe response. Although it is a reasonable assumption, uncertainties might still exist.

8. Conclusions

This study deals with the evaluation of 1-hour short-term extreme response in association with the use of environmental contour method to determine long-term extreme structural responses and associated uncertainties for an end-anchored curved floating bridge. The floating bridge considered is about 4600 m long and was an early concept for crossing the Bjørnafjord. The long-term extreme responses are estimated by using the response at a 90% fractile of a representative short term condition.

The short-term environmental conditions (ECs) that cause the largest extreme responses, i.e.

EC2 with combined wind and wave condition, are determined based on an early version of the metocean design basis for the fjord. EC1 with wave only condition is also studied for the reference. A total of 100 1h samples are simulated for each EC to predict the extreme responses. The extreme responses are expressed as $\mu + \kappa\sigma$, where μ and σ are the ensemble mean and standard deviation, and κ is a multiplying factor.

Statistical analyses indicate that the structural responses are likely to be Gaussian distributed. A simplified analytical method is thus used to predict the factor κ based on the zero up-crossing periods and bandwidth parameters estimated from ensemble averaged spectral moments. Two extrapolation methods, including the Gumbel method and the mean upcrossing rate (MUR) method, are also employed to predict the factor κ.

The multiplying factor κ for axial force F_x, strong axis bending moment M_z and weak axis bending moment M_y of the bridge girder are found to be in the vicinity of 4. Compared to the Gumbel method, the simplified method can give an overall good prediction of multiplying factor κ for F_x, M_z and M_y, with a discrepancy less than 4%. However, large discrepancy will occur for non-Gaussian distributed responses and/or extremely narrow-banded responses. The κ estimated by the Gumbel method, the MUR method and the simplified method are generally close but with discrepancies.

Uncertainties in the extreme value prediction are also addressed in the study, including statistical uncertainties due to a limited number of simulations and model uncertainties due to approaches for extreme value prediction, etc. In general, the smaller the ensemble number, the larger the statistical uncertainties.

Based on the results of 10 sets of 10 1-h ensembles, the mean and coefficient of variation (CoV) of μ, κ, σ and extremes of F_x and M_z under EC1 and EC2 are evaluated. The CoV of μ is fairly small, less than 0.04; while the CoV of σ is less than 0.045. The CoV of κ is relatively large, mainly between 3.5×10^{-2} and 6.5×10^{-2}. Moreover, μ, κ and σ are statistically independent, the CoV of extreme is a function of the mean and CoV of μ, κ and σ. The CoV of extremes estimated by the simplified analytical method is fairly small, less than 0.035. While the CoV of extremes estimated by the Gumbel and MUR methods are much larger and can reach 0.137 and 0.158, respectively.

In the practical design of floating bridges, only a limited number of simulations (e.g. 10) is used to predict the extreme structural responses. To account for the statistical uncertainty due to a limited number of simulations, a correction factor should be employed in order to achieve a conservative estimation of extreme. A procedure to derive the correction factor is presented in this study. For the floating bridge considered, if only 10 1-h simulations are simulated for extreme value prediction, the correction factor is recommended to be 1.1 when the absolute value of mean μ is smaller than σ, and be 1.2 when the absolute value of mean μ is larger than σ, in order to achieve a 90% conservative estimation of extreme.

As a whole, this study addresses the estimation of long-term extreme responses and associated uncertainties for an extra-long floating bridge by using an engineering approach, i.e., the environmental contour method. It gives insights on the extreme behavior of floating bridges and also provides a simplified procedure to deal with statistical uncertainty due to a limited number of simulations. These approaches are also applicable and useful for other floating bridges, in terms of prediction of extreme responses for ULS design check. The present study cannot conclude the accuracy of these three methods, since the exact value of long-term extreme response is not known yet. This can be studied by carrying out a full long-term analysis, but it is not the focus of the present study and can be a future work.

Acknowledgment

This work was supported by the Norwegian Public Roads Administration and in parts by the Research Council of Norway through the Centre for Ships and Ocean Structures (CeSOS) and Centre for Autonomous Marine Operations and Systems (AMOS), at the Department of Marine Technology, NTNU, Trondheim, Norway. The support is gratefully acknowledged by the authors. The first author would also like to appreciate the support from the Thousand Young Talent Plan Project, the State Key Laboratory of Ocean Engineering and the research startup fund of Shanghai Jiao Tong University, Shanghai, China.

Appendix

A. Propagation of error

Considering a function that is expressed as

$$f(a, b, c) = c + a \cdot b \tag{19}$$

where a, b and c are random variables. Assuming that the mean value of a, b and c are denoted by μ_a, μ_b and μ_c, and their standard deviation by σ_a, σ_b and σ_c, respectively. Their coefficient of variations (CoV) are denoted by CoV_a, CoV_b and CoV_c, respectively. Here we have $\sigma_a = \mu_a \cdot CoV_a$, $\sigma_b = \mu_b \cdot CoV_b$ and $\sigma_c = \mu_c \cdot CoV_c$

The standard error of $g = a \cdot b$ is estimated by

$$\sigma_g^2 = (\frac{\partial g}{\partial a})^2 \sigma_a^2 + (\frac{\partial g}{\partial b})^2 \sigma_b^2 + 2(\frac{\partial g}{\partial a})(\frac{\partial g}{\partial b})\sigma_{ab}^2 \tag{20}$$

where σ_{ab} is the covariance of a and b. $\frac{\partial g}{\partial a}$ and $\frac{\partial g}{\partial b}$ are evaluated at the mean value. If a and b are uncorrelated, $\sigma_{ab} = 0$. This yields

$$(\frac{\sigma_g}{\mu_a \cdot \mu_b})^2 = (\frac{\sigma_a}{\mu_a})^2 + (\frac{\sigma_b}{\mu_b})^2 \tag{21}$$

The standard error of function f is then given by

$$\sigma_f = \sqrt{\sigma_c^2 + \sigma_g^2} = \sqrt{\sigma_c^2 + \mu_a^2 \cdot \sigma_b^2 + \mu_b^2 \cdot \sigma_a^2} = |\mu_a \cdot \mu_b| \sqrt{(\frac{\mu_c}{\mu_a \cdot \mu_b})^2 \cdot CoV_c^2 + CoV_b^2 + CoV_a^2} \tag{22}$$

Its coefficient of variation is approximated by

$$CoV_f = \frac{|\mu_a \cdot \mu_b|}{\mu_a \cdot \mu_b + \mu_c} \sqrt{(\frac{\mu_c}{\mu_a \cdot \mu_b})^2 \cdot CoV_c^2 + CoV_b^2 + CoV_a^2} \tag{23}$$

B. Accuracy of extremes due to a limited number of simulations

Let the extreme values predicted by M sets of simulations be $x_i, i = 1, 2, ..., M$. The final estimate of this extreme, say S, will be [31]:

$$S = \frac{1}{M} \sum_{i=1}^{M} x_i \tag{24}$$

if μ is the exact ensemble average of this extreme, such that $\mu = E[x_i]$, then the error in the estimate S will be:

$$\epsilon = S - \mu \tag{25}$$

where ϵ is a random variable. Considering the statistics of the error ϵ, the average value of ϵ is given by:

$$E[\epsilon] = \frac{1}{M} \sum_{i=1}^{M} E[x_i] - \mu = 0 \tag{26}$$

and the mean squared value of ϵ is:

$$E[\epsilon^2] = \frac{1}{M^2} \sum_{i=1}^{M} \sum_{j=1}^{M} E[x_i x_j] - \frac{2\mu}{M} \sum_{i=1}^{M} E[x_i] + \mu^2 = \frac{1}{M^2} \sum_{i=1}^{M} E[x_i^2] + \frac{2}{M^2} \sum_{i=1}^{M} \sum_{j=i+1}^{M} E[x_i x_j] - \frac{2\mu}{M} \sum_{i=1}^{M} E[x_i] + \mu^2 \tag{27}$$

Noting that the terms x_i are statistically independent, and defining σ such that $E[x_i^2] = \sigma^2 + \mu^2$, Eq. 27 can be written as

$$E[\epsilon^2] = \frac{1}{M}(\sigma^2 + \mu^2) + \frac{1}{M}(M-1)\mu^2 - 2\mu^2 + \mu^2 = \frac{\sigma^2}{M} \tag{28}$$

The root mean square error of the estimate S, say δ, will now be written as:

$$\delta = \frac{1}{\sqrt{M}} \frac{\sigma}{\mu} \tag{29}$$

References

[1] T. Moan, M. E. Eidem, Floating bridges and submerged tunnels in norway—the history and future outlook, in: C. M. Wang, S. H. Lim, Z. Y. Tay (Eds.), WCFS2019. Lecture Notes in Civil Engineering, vol 41., Springer, 2020 (2020).

[2] Z. Cheng, Z. Gao, T. Moan, Hydrodynamic load modeling and analysis of a floating bridge in homogeneous wave conditions, Marine Structures 59 (2018) 122–141 (2018).

[3] Z. Cheng, Z. Gao, T. Moan, Numerical modeling and dynamic analysis of a floating bridge subjected to wind, wave, and current loads, Journal of Offshore Mechanics and Arctic Engineering 141 (1) (2019) 011601 (2019).

[4] K. A. Kvåle, R. Sigbjörnsson, O. Øiseth, Modelling the stochastic dynamic behaviour of a pontoon bridge: a case study, Computers & Structures 165 (2016) 123–135 (2016).

[5] Z. Cheng, Z. Gao, T. Moan, Wave load effect analysis of a floating bridge in a fjord considering inhomogeneous wave conditions, Engineering Structures 163 (2018) 197–214 (2018).

[6] A. Naess, T. Moan, Stochastic dynamics of marine structures, Cambridge University Press, Cambridge, UK, 2013 (2013).

[7] S. R. Winterstein, T. C. Ude, C. A. Cornell, P. Bjerager, S. Haver, Environmental parameters for extreme response: Inverse form with omission factors, in: Proceedings of the ICOSSAR-93, Innsbruck, Austria, 1993, pp. 551–557 (1993).

[8] S. Haver, S. R. Winterstein, Environmental contour lines: A method for estimating long term extremes by a short term analysis, Transactions of the Society of Naval Architects and Marine Engineers 116 (2009) 116–127 (2009).

[9] S. R. Winterstein, K. Engebretsen, Reliability-based prediction of design loads and responses for floating ocean structures, in: 17 th International Conference on Offshore Mechanics and Arctic Engineering, Lisbon, Portugal, 1998, p. 1998 (1998).

[10] DNV GL, Environmental conditions and environmental loads (DNV-RP-C205), Det Norske Veritas AS, Oslo, Norway (2014).

[11] NORSOK N-003, Actions and action effects, Norwegian Technology Standard, Oslo, Norway (2017).

[12] A. Naess, O. Gaidai, P. S. Teigen, Extreme response prediction for nonlinear floating offshore structures by Monte Carlo simulation, Applied Ocean Research 29 (4) (2007) 221–230 (2007). doi:10.1016/j.apor.2007.12.001.

[13] A. Naess, O. Gaidai, Monte Carlo Methods for Estimating the Extreme Response of Dynamical Systems, Journal of Engineering Mechanics 134 (8) (2008) 628–636 (2008). doi:10.1061/(ASCE)0733-9399(2008)134:8(628).

[14] N. Saha, Z. Gao, T. Moan, A. Naess, Short-term extreme response analysis of a jacket supporting an offshore wind turbine, Wind Energy 17 (1) (2014) 87–104 (2014).

[15] Z. Cheng, H. A. Madsen, W. Chai, Z. Gao, T. Moan, A comparison of extreme structural responses and fatigue damage of semi-submersible type floating horizontal and vertical axis wind turbines, Renewable Energy 108 (2017) 207–219 (2017). doi:10.1016/j.renene.2017.02.067.

[16] O. Øiseth, A. Rönnquist, A. Naess, R. Sigbjömsson, Estimation of extreme response of floating bridges by monte carlo simulation, in: Proceedings of the 9th International Conference on Structural Dynamics, EURODYN 2014, Porto, Portugal, 2014 (2014).

[17] F.-I. G. Giske, K. A. Kvåle, B. J. Leira, O. Øiseth, Long-term extreme response analysis of a long-span pontoon bridge, Marine Structures 58 (2018) 154–171 (2018). doi:https://doi.org/10.1016/j.marstruc.2017.11.010.

[18] Y. Xu, O. Øiseth, T. Moan, A. Naess, Prediction of long-term extreme load e ff ects due to wave and wind actions for cable-supported bridges with fl oating pylons, Engineering Structures 172 (2018) 321–333 (2018).

[19] T. Moan, Z. Gao, E. Ayala-Uraga, Uncertainty of wave-induced response of marine structures due to long-term variation of extratropical wave conditions, Marine Structures 18 (4) (2005) 359–382 (2005).

[20] COWI, NOT-HYDA-018 Curved bridge navigation channel in south - environmental loading analysis., Report for the Norwegian Public Road Administration. COWI AS, Oslo, Norway (2016).
URL https://www.vegvesen.no/_attachment/1605060/binary/1145259?fast_title=Bj%C3%B8rnafjorden+Endeforankret+flytebun+-+Oppsumering+av+analyser.pdf

[21] MARINTEK, Rifelx theory manual, version 4.0 (2012).

[22] E. Strømmen, Theory of bridge aerodynamics, Springer Science & Business Media, 2010 (2010).

[23] MARINTEK, Simo-theory manual version 4.0 (2012).

[24] O. M. Faltinsen, Sea loads on ships and offshore structures, Cambridge University Press, Cambridge, UK, 1995 (1995).

[25] E. H. Vanmarcke, On the distribution of the first-passage time for normal stationary random processes, Journal of Applied Mechanics (1975) 215–220 (1975).

[26] I. Papaioannou, R. Gao, E. Rank, C. M. Wang, Stochastic hydroelastic analysis of pontoon-type very large floating structures considering directional wave spectrum, Probabilistic Engineering Mechanics 33 (2013) 26–37 (2013).

[27] Statens Vegvesen, Design basis metocean, SBJ-01-C3-SVV-01-BA-001, Statens Vegvesen, norway (2017).

[28] Z. Cheng, E. Svangstu, T. Moan, Z. Gao, Long-term joint distribution of environmental conditions in a norwegian fjord for design of floating bridges, prepared for possible journal publication (2019).

[29] B. J. Jonkman, Turbsim user's guide: Version 1.50., Tech. rep. (2009).

[30] Statens Vegvesen, Håndbok N400, Bruprosjektering, Statens Vegvesen, Norway (2015).

[31] R. Langley, On the time domain simulation of second order wave forces and induced responses, Applied ocean research 8 (3) (1986) 134–143 (1986).

[32] M. J. Tucker, E. G. Pitt, Waves in ocean engineering, no. Elsevier, 2001 (2001).

[33] Z. Cheng, E. Svangstu, Z. Gao, T. Moan, Field measurements of inhomogeneous wave conditions in Bjørnafjorden, Journal of Waterway, Port, Coastal, and Ocean Engineering 145 (1) (2019) 05018008 (2019).